Highly Regiospecific Zirconocene Catalysts for the Isospecific Polymerization of Propene

Luigi Resconi,*,† Fabrizio Piemontesi,† Isabella Camurati,† Olof Sudmeijer,‡ Ilya E. Nifant'ev,*,§ Pavel V. Ivchenko,§ and Lyudmila G. Kuz'mina||

Contribution from the Montell Polyolefins, Centro Ricerche G. Natta, 44100 Ferrara, Italy, Shell Research and Technology Centre, 1031 CM Amsterdam, The Netherlands, Department of Chemistry, Moscow University, 119899 Moscow, Russia, and Institute of General and Inorganic Chemistry, Russian Academy of Sciences, 117907 Moscow, Russia

Received September 9, 1997

Abstract: A new class of isospecific and highly regiospecific *C_2-symmetric ansa*-zirconocenes, characterized by a bisindenyl ansa ligand with bulky substituents in the 3 position of indene *and* a single carbon bridge is disclosed: variation of the size of the substituent in C(3) has a strong effect on the extent of chain transfer and isospecificity in propene polymerization. In fact, while *rac*-[Me_2C(1-indenyl)$_2$]$ZrCl_2$ produces low molecular weight and moderately isotactic polypropene (iPP) also containing some regioirregularities ($\bar{M}_n$ = 6500, *mmmm* ca. 81% and $2,1_{tot}$ = 0.4% at 50 °C in liquid monomer), *rac*-[Me_2C(3-*tert*-butyl-1-indenyl)$_2$]$ZrCl_2$ produces iPP with molecular weights between 25 000 (T_p = 70 °C) and 410 000 (T_p = 20 °C) and a fairly high isotacticity (*mmmm* ca. 95% at 50 °C), with no detectable 2,1 units. The influence of polymerization temperature on the catalyst performance has been investigated by polymerizing liquid propene in the temperature range of 20−70 °C: the experimental $\Delta\Delta E^{\ddagger}$ values for enantioface selectivity have been estimated for two members of the new class (*rac*-[Me_2C(3-*tert*-butyl-1-indenyl)$_2$]$ZrCl_2$ $\Delta\Delta E^{\ddagger}_{enant}$ = 4.6 kcal/mol; *rac*-[Me_2C(3-(trimethylsilyl)-1-indenyl)$_2$]$ZrCl_2$ $\Delta\Delta E^{\ddagger}_{enant}$ = 2.6 kcal/mol). For comparison, Brintzinger's moderately isospecific, benchmark catalyst *rac*-[ethylene(1-indenyl)$_2$]$ZrCl_2$ ($\Delta\Delta E^{\ddagger}_{enant}$ = 3.3 kcal/mol), the single carbon bridged, unsubstituted *rac*-[Me_2C(1-indenyl)$_2$]$ZrCl_2$ ($\Delta\Delta E^{\ddagger}_{enant}$ = 2.8 kcal/mol), and the C_2-symmetric, practically aspecific, *rac*-[ethylene(3-methyl-1-indenyl)$_2$]$ZrCl_2$ ($\Delta\Delta E^{\ddagger}_{enant}$ = 1.9 kcal/mol) are also reported. The molecular structures of *rac*-[Me_2C(3-*tert*-butyl-1-indenyl)$_2$]$ZrCl_2$ and *rac*-[Me_2C(3-(trimethylsilyl)-1-indenyl)$_2$]$ZrCl_2$ have been determined.

Introduction

The molecular architecture of polypropenes obtained from *ansa*-zirconocenes is strongly dependent on the biscyclopentadienyl ligand structure.[1] Since the early *C_2-symmetric*, racemic *ansa*-metallocenes for the isospecific polymerization of olefins, several different classes of such catalysts have been developed.

The prototypal class based on *C_2-symmetric* racemic zirconocenes with *ansa*-bis(3-alkyl-cyclopentadienyl) or *ansa*-bis-(indenyl) ligands (I in Chart 1) produce isotactic polypropenes (iPP) with isotacticities ranging from very low to quite high, but invariably with low molecular weights,[1,2] the best known example being Brintzinger's *rac*-[ethylene(1-indenyl)$_2$]$ZrCl_2$.[3] The introduction of an alkyl substituent in the 2 position (α to the bridge) of either an *ansa*-bis(3-alkylcyclopentadienyl)[4] or *ansa*-bis(indenyl)[5] zirconium complex (II in Chart 1) increases both the stereoregularity and the molecular weight of the produced polyolefin, and reduces the amount of regioirregularities, in comparison with the unsubstituted analogue. Well-known examples are Me_2Si(2,4-dimethylcyclopentadienyl)$_2ZrCl_2$,[4] Me_2Si(2-methylindenyl)$_2ZrCl_2$,[5] which led to the recent important development of the first zirconocenes able to compete with the performance of industrial Ti-based catalysts,[6] and Me_2Si-(2-methylbenz[*e*]indenyl)$_2ZrCl_2$.[7]

The above racemic catalysts are almost invariably generated along with their *meso* forms which produce unwanted low molecular weight atactic polypropene with nonnegligible po-

† Montell Polyolefins.
‡ Shell Research and Technology Centre.
§ Moscow University.
|| Russian Academy of Sciences.

(1) (a) Ewen, J. A.; Haspeslagh, L.; Elder, M. J.; Atwood, J. L.; Zhang, H.; Cheng, H. N. In *Transition Metals and Organometallics as Catalysts for Olefin Polymerization*; Kaminsky, W., Sinn, H., Eds.; Springer-Verlag: Berlin, 1988; p 281. (b) Ewen, J. A.; Elder, M. J.; Jones, R. L.; Haspeslagh, L.; Atwood, J. L.; Bott, S. G.; Robinson, K. *Makromol. Chem., Macromol. Symp.* **1991**, *48/49*, 253. (c) Spaleck, W.; Antberg, M.; Dolle, V.; Klein, R.; Rohrmann, J.; Winter, A. *New J. Chem.* **1990**, *14*, 499. (d) Brintzinger, H. H.; Fischer, D.; Mülhaupt, R.; Rieger, B.; Waymouth, R. M. *Angew. Chem., Int. Ed. Engl.* **1995**, *34*, 1143.

(2) Collins, S.; Gauthier, W. J.; Holden, D. A.; Kuntz, B. A.; Taylor, N. J.; Ward, D. G. *Organometallics* **1991**, *10*, 2061.

(3) (a) Wild, F.; Wasiucionek, M.; Huttner, G.; Brintzinger, H. H. *J. Organomet. Chem.* **1985**, *288*, 63. (b) Collins, S.; Kuntz, B.; Taylor, N.; Ward, D. *J. Organomet. Chem.* **1988**, *342*, 21. (c) Lee, J.; Gauthier, W.; Ball, J.; Iyengar, B.; Collins, S. *Organometallics* **1992**, *11*, 2115. (d) Piemontesi, F.; Camurati, I.; Resconi, L.; Balboni, D.; Sironi, A.; Moret, M.; Zeigler, R.; Piccolrovazzi, N. *Organometallics* **1995**, *14*, 1256.

(4) Mise, T.; Miya, S.; Yamazaki, H. *Chem. Lett.* **1989**, 1853. Roll, W.; Brintzinger, H. H.; Rieger, B.; Zolk, R. *Angew. Chem., Int. Ed. Engl.* **1990**, *29*, 279.

(5) Spaleck, W.; Antberg, M.; Rohrmann, J.; Winter, A.; Bachmann, B.; Kiprof, P.; Behm, J.; Herrmann, W. *Angew. Chem., Int. Ed. Engl.* **1992**, *31*, 1347−1350.

(6) Spaleck, W.; Küber, F.; Winter, A.; Rohrmann, J.; Bachmann, B.; Antberg, M.; Dolle, V.; Paulus, E. *Organometallics* **1994**, *13*, 954.

(7) (a) Stehling, U.; Diebold, J.; Kirsten, R.; Röll, W.; Brintzinger, H.-H.; Jüngling, S.; Mülhaupt, R.; Langhauser, F. *Organometallics* **1994**, *13*, 964. (b) Jüngling, S.; Mülhaupt, R.; Stehling, U.; Brintzinger, H. H.; Fischer, D.; Langhauser, F. *J. Polym. Sci., Part A: Polym. Chem.* **1995**, *33*, 1305.

S0002-7863(97)03160-0 CCC: $15.00
Published on Web 03/03/1998

Chart 1

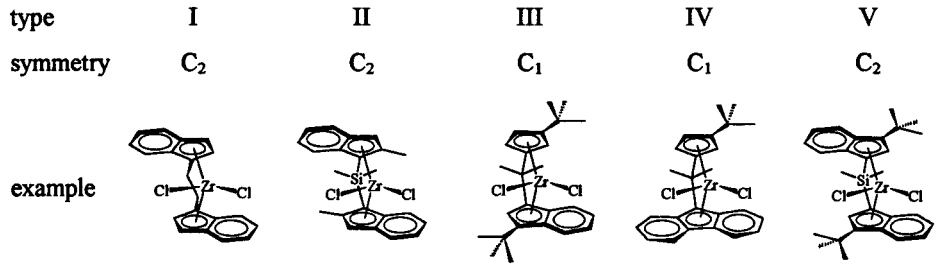

Scheme 1

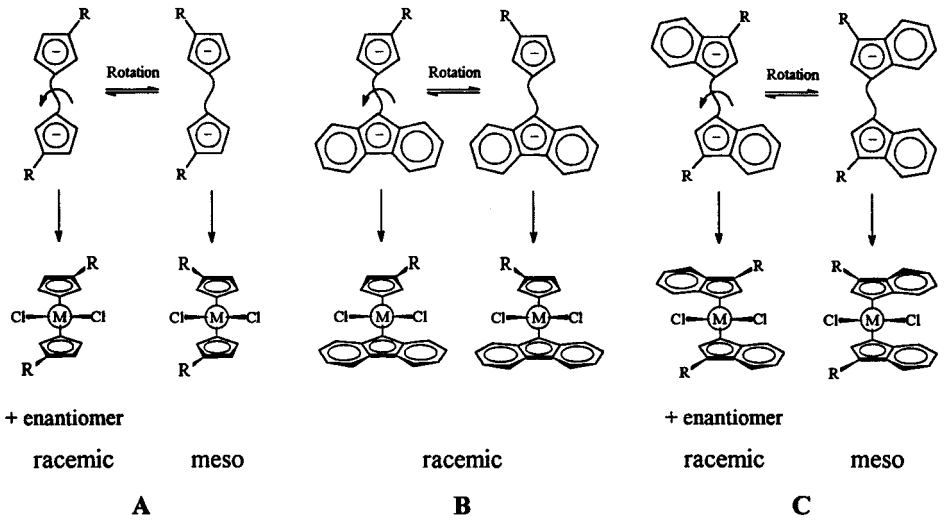

lymerization activity and are difficult to remove from the catalyst mixture (Scheme 1, A). In addition, all of these modified *C_2-symmetric* systems require multistep, low overall yield synthetic routes.[6,7]

Miyake has developed a class of C_1-symmetric systems[8] (III in Chart 1) which are highly isospecific (e.g., *threo*-Me_2C(3-*tert*-butylcyclopentadienyl)(3-*tert*-butylindenyl)$ZrCl_2$) but again produce low molecular weight iPP. In this case, the meso-like (erythro) isomer (less active than the racemic one) is partially isospecific. Marks[9] and Ewen[10] have designed a notable class of C_1-symmetric systems (IV in Chart 1) for which a *meso* form does not exist (Scheme 1, B). Ewen's elegant catalyst design, Me_2C(3-*tert*-butyl-1-cyclopentadienyl)(9-fluorenyl)$ZrCl_2$, also includes an easy ligand synthesis. This catalyst, however, has a relatively low stereoselectivity (*mmmm* = 78% at 40 °C)[11] and, again, produces iPP with modest molecular weights. Its Me_2Si-bridged analogue shows a better performance.[10]

Ewen has also proposed a novel type (V in Chart 1) of *C_2-symmetric* systems, constituted of metallocenes having two strapped indenyls with a bulky substituent in the 3 position of indene.[12] The prototype of this class, *rac*-Me_2Si(3-*tert*-butyl-1-indenyl)$_2ZrCl_2$, which reintroduces the problem of meso isomer formation (Scheme 1, C), was reported by Miyake[8] to have a very poor performance, both in terms of stereospecificity and molecular weights (*mmmm* = 75.5 and M_w = 5000 only, even at the low T_p of 1 °C), even if compared to that of the early *C_2-symmetric* zirconocenes.

Scheme 2

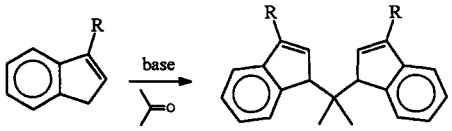

At the same time, we were also investigating the effect of the alkyl substituent in zirconocenes of the latter type. Some of us had developed a simple, inexpensive, and general synthesis of single carbon bridged ligands, from acetone and indene (Scheme 2).[13]

The ligand dianions of this class generate zirconocenes in high yield, and the synthesis can be made diastereoselective by the use of stannylated ligands.[14]

We have investigated the performance of two members of the above class of zirconocene catalysts,[15] namely *rac*-[isopropylidenebis(3-*tert*-butyl-1-indenyl)]zirconium dichloride (*rac*-$Me_2C(3\text{-}^tBu\text{-}Ind)_2ZrCl_2$, **4**) and *rac*-[isopropylidenebis(3-(trimethylsilyl)-1-indenyl)]zirconium dichloride (*rac*-$Me_2C(3\text{-}Me_3Si\text{-}1\text{-}Ind)_2ZrCl_2$ **5**), and report here their synthesis, characterization, and evaluation in the methylalumoxane (MAO)-cocatalyzed polymerization of propene. To put the performance of **4** and **5** in the proper perspective, the *C_2-symmetric*, moderately isospecific *rac*-[ethylenebis(1-indenyl)]$ZrCl_2$ (**1**)[3] and *rac*-[isopro-

(8) Miyake, S.; Okumura, Y.; Inazawa, S. *Macromolecules* **1995**, *28*, 3074.

(9) Giardello, M.; Eisen, M.; Stern, C. L.; Marks, T. J. *J. Am. Chem. Soc.* **1995**, *117*, 12114.

(10) Ewen, J. A.; Elder, M. J. In *Ziegler Catalysts*; Fink, G., Mülhaupt, R., Brintzinger, H. H., Eds.; Springer-Verlag: Berlin, 1995; p 99.

(11) Razavi, A.; Vereecke, D.; Peters, L.; Den Dauw, K.; Nafpliotis, L.; Atwood, J. L. In *Ziegler Catalysts*; Fink, G., Mülhaupt, R., Brintzinger, H. H., Eds.; Springer-Verlag: Berlin, 1995; p 111.

(12) Ewen, J. A. *Macromol. Symp.* **1995**, *89*, 181.

(13) Nifant'ev, I. E.; Ivchenko, P. V. Eur. Pat. Appl. 722 949 (to Montell). Nifant′ev, I. E.; Ivchenko, P. V.; Kuz'mina, L. G.; Luzikov, Yu., N.; Sitnikov, A. A.; Sizan, O. E. *Synthesis* **1997**, 469.

(14) Nifant′ev, I. E.; Ivchenko, P. V.; Resconi, L. Eur. Pat. Appl. 722,-950 (to Montell); *Chem. Abstr.* **1996**, *125*, 196000. Nifant'ev, I. E.; Ivchenko, P. V. *Organometallics* **1997**, *16*, 713.

(15) Resconi, L.; Piemontesi, F.; Nifant'ev, I. E.; Ivchenko, P. V. PCT Int. Appl. WO 96 22, 995 (to Montell); *Chem. Abstr.* **1996**, *125*, 222171.

Chart 2

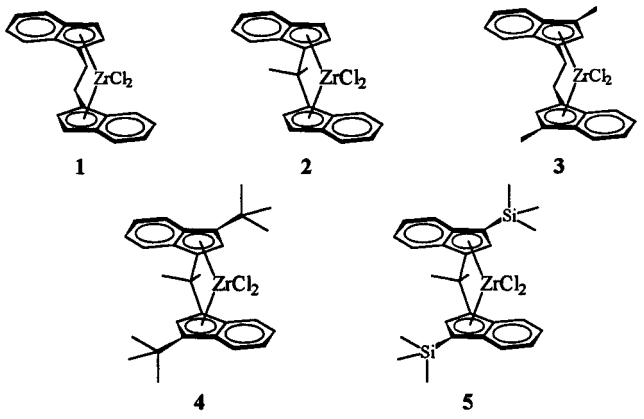

pylidenebis(1-indenyl)]$ZrCl_2$ (**2**),[1c] and the aspecific *rac*-[ethylenebis(3-methyl-1-indenyl)]$ZrCl_2$ (**3**)[1a] (Chart 2) are used as benchmarks.

Results

1. Synthesis of the Zirconocenes. Compounds **1**−**3** were synthesized as described in the literature. 2,2-bis(indenyl)-propane and 2,2-bis(3-*tert*-butyl-1-indenyl)propane ligand precursors were synthesized according to the procedure developed by one of us[13] by direct condensation of indene or 3-*tert*-butylindene and acetone. For the purpose of their purification, the crude products were converted into their dilithium salts.[13] 2,2-Bis(1-(trimethylsilyl)-3-indenyl)propane was prepared by silylation of the dilithium salt of bis-indenyldimethylmethane according to the procedure described in ref 14.

Compounds **4** and **5** were prepared by transmetalation between the bis-trialkyltin derivative of the ligands and $ZrCl_4$ in noncoordinating solvents (Scheme 3).[14]

In a one-pot synthesis, the dilithium salts of 2,2-bis-(alkylindenyl)propanes (alkyl = ^{t}Bu, Me_3Si) were treated with Me_3SnCl in Et_2O to give quantitatively 2,2-bis(1-(trimethyl-stannyl)-1-alkyl-3-indenyl)propanes which were then (after removing Et_2O) reacted with $ZrCl_4$ in toluene to give **4** and **5** (Scheme 3). The intermediate distannyl derivatives **6** and **7** consist of rac/meso mixtures that can be easily identified by ^{1}H NMR: the isopropylidene bridge serves as a stereochemical probe for identifying the meso (diastereotopic methyls) and racemic (identical methyls) isomers.

Surprisingly, **6** and **7** do not consist of equal amounts of rac and meso forms as we had observed in the synthesis of the related 1,2-bis(1-(trimethylsilyl)-4,7-dimethyl-3-indenyl)ethane, for which the dilithium or dipotassium salt, generated in THF, was quenched directly with Me_3SiCl without the need of prior isolation.[16] On the contrary, *rac*-**6** and *rac*-**7** were found to be the major isomers in their reaction mixtures. It is remarkable that the rac/meso distributions of distannyl derivatives depend on the crystallization method of the initial dilithium salts. In general, the *rac*-**6**/*meso*-**6** ratio varies in the range 1.5−2.0:1 and *rac*-**7**/*meso*-**7** in the range 1.0−1.2:1. This effect is probably caused by the existence of nonionic interactions between Li atoms and indenyl fragments in the crystalline salts. Cases of such structures−metallocene-like lithium salts−have been recently reported.[17]

Yields of **4** and **5** are close to 90%. Evidently, the rac/meso ratio for the zirconocenes reproduces that of the starting distannyl derivatives. Therefore, the real chemical yield (from the ligand) of *rac*-**4** is considerably more than 50%. Unfortunately, the similarity of physical properties for rac and meso isomers of **4** and **5** makes their separation rather difficult; rac and meso forms of **4** and **5** were recrystallized from DME, in which the racemic isomers were slightly less soluble.

We found that the stabilities of **4** and **5** depend strongly on their purity. Chemically pure samples could be exposed to air for 10 h without noticeable decomposition, while the samples contaminated with even small amounts of tin-containing impurities underwent extensive decomposition in just a few minutes. Complexes **4** and **5** could be prepared directly from the corresponding dilithium salts as well. Although the yields of zirconocenes were quite high (70−80%), 1:1 rac/meso mixtures of **4** and **5** were obtained.

The major advantage of these novel systems resides in the very easy, high-yield synthetic procedure, especially the 2,2-bis(3-alkyl-1-indenyl)propane ligand precursors. In addition, an added advantage of these compounds is the presence of an isopropylidene bridge which, as mentioned above for the distannyl derivatives, represents a builtin, very convenient stereochemical probe for identifying the meso (diastereotopic methyls) and racemic (identical methyls) zirconocene isomers.

Scheme 3

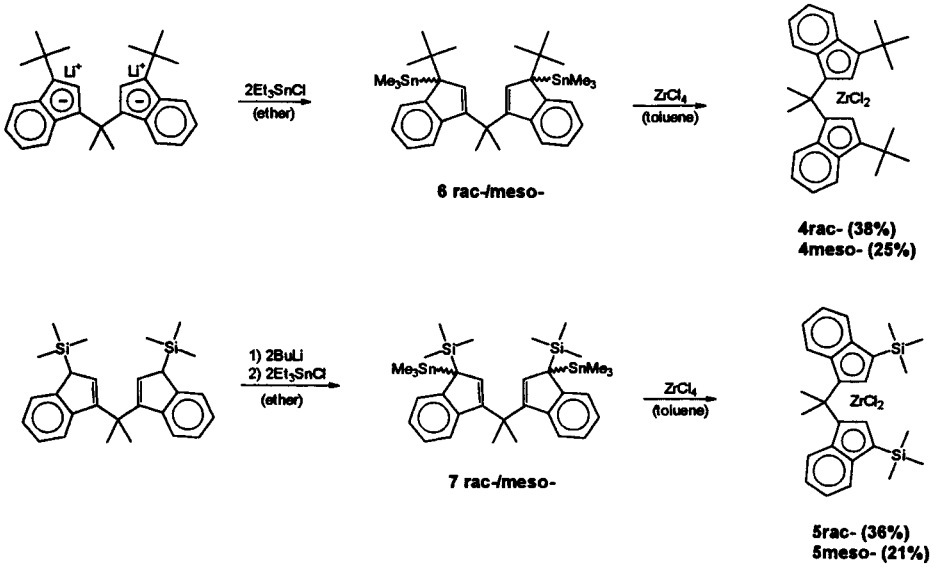

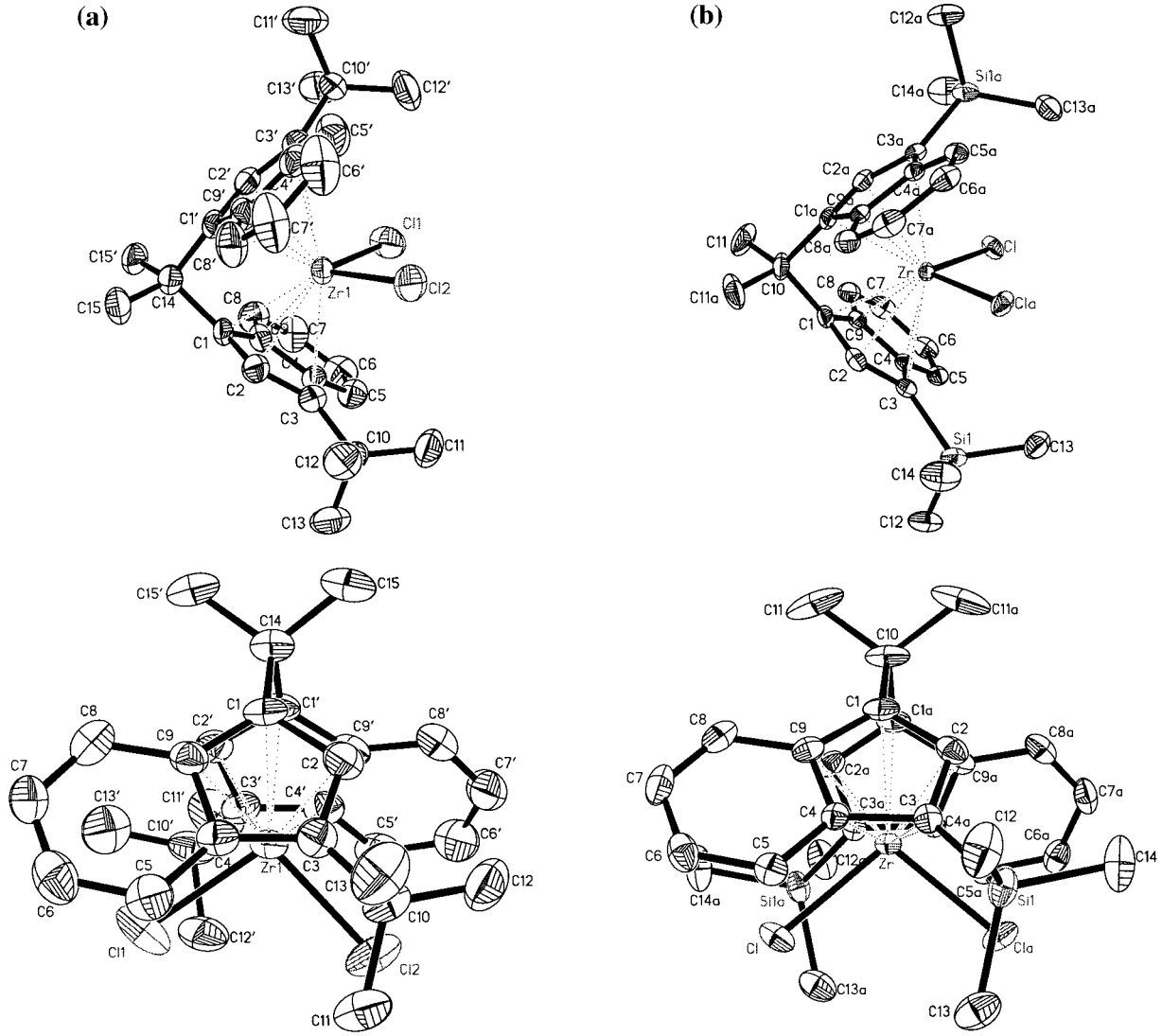

Figure 1. (a) Molecular structure and labeling scheme for *rac*-$Me_2C(3\text{-}^t\text{Bu-Ind})_2ZrCl_2$ (**4**). (b) Molecular structure and labeling scheme for *rac*-$Me_2C(3\text{-}Me_3Si\text{-Ind})_2ZrCl_2$ (**5**).

This stereochemical probe is obviously present also in the Me_2-Si-bridged zirconocenes but is lacking in the related ethylene bridged zirconocenes such as **1** and **3**.

2. X-ray Analysis of 4 and 5. The racemic structures of **4** and **5** were confirmed by X-ray analysis. Two views of each are shown in Figure 1. The zirconium atom is coordinated to the η^5 cyclopentadienyl fragments of the two indenyls of the ansa ligand and two chlorine atoms. Mutual arrangement of the indenyl fragments corresponds to C_2 symmetry, which is geometrically rigorous for **5**.

The molecules show noticeable distortions due to the short isopropylidene bridge. The most relevant geometrical parameters for **4** and **5** and a series of bis(cyclopentadienyl) zirconium complexes are compared in Table 1. In **4** and **5**, the inner angle (ϕ, see Chart 3) at the bridging carbon atom (100.1(5)° for **4** and 99.4(2)° for **5**) lies within the range 99.0−100.3° characteristic of other *ansa*-biscyclopentadienyl complexes with a single carbon bridge (**2**, **2m**, and **b**−**d**).

The angles γ between each $C_{Cp}-C_{br}$ bond and the plane of the corresponding cyclopentadienyl fragment are equal to 13.6° and 11.4° in **4** and 13.2° (both) in **5**. These values are close to those (12.6−15.1°) in **2**, **2m**, and **b**−**d**. It is of interest that the angle ϕ at the bridging atom ranges within 94.3° and 95.2°, and the displacement angle γ from the Cp planes varies from 16.0° to 18.1° in ansa complexes with a Si bridge such as **a**. In **a** (and other Si-bridged complexes), a smaller *ansa* ϕ angle and a larger γ angle compared to those in **4** and **2**, **2m**, and **b**−**d**, result in less significant distortion of other geometrical parameters.

The α angle cp−Zr−cp′ (cp, cp′ = centroids of the Cp rings) of 118.3° for **4** and 117.4° for **5** is close to those in **2** and **2m** (117.9−118.3°) and somewhat larger than in **b**−**d** (115.6−117.1°). It should be noted that, in bis(cyclopentadienyl)-zirconium compounds without a bridge between the two Cp rings (**e**−**g**), this parameter ranges from 129.0° to 132.5°.

An important descriptor of bent metallocene structures is the angle between the Cp plane and the cp−Zr bond, δ (Chart 3), which gives an idea (together with the value of the β angle) of the accessibility of the metal atom: the lower the values are from 90°, the more the metal is tucked in the ligand envelope.

The main geometrical distinction of **4** from **2**, **2m**, and **b**−**d** is associated with the angle β and the range of $Zr-C_{Cp}$ bond distances. In **4**, β (75.2°) is increased compared to those of **2**, **2m**, and **b**−**d** (70.9−71.8°). On the contrary, **5** has a dihedral angle β that falls closer to the range of the other complexes. The range of $Zr-C_{Cp}$ bond distances (Δr = 0.25 Å) is wider

(16) Resconi, L.; Piemontesi, F.; Camurati, I.; Balboni, D.; Sironi, A.; Moret, M.; Rychlicki, H.; Zeigler, R. *Organometallics* **1996**, *15*, 5046.

Table 1. Relevant Geometrical Parameters (deg or Å) of Selected Cp'_2ZrX_2 Complexes (see Chart 3 for angle labels)

N°	Molecule	ϕ	α	γ	β	δ	r(Zr-C_{Cp}); Δr (Å)	Ref.
1	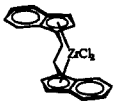		125.3	-1.8, 1.2	60.4	87.2	2.44-2.62; 0.18	3a
2	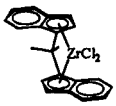	100.3	118.2	14.6	70.9	85.5	2.44-2.62; 0.18	18
2m	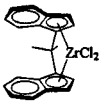	100.1 100.1	118.3 117.9	14.3; 14.5 14.5; 14.2	71.7 71.5	85.0 85.3	2.43-2.63; 0.20 2.43-2.61; 0.18	18
4	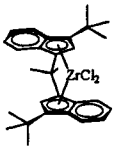	100.1	118.3	13.6; 11.4	75.2	83.3	2.43-2.68; 0.25	This work
5	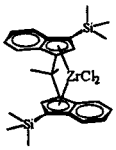	99.4	117.4	13.2	72.6	85.0	2.45-2.65; 0.20	This work
a	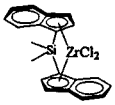	94.4	127.8	17.4; 16.8	60.2	85.7	2.46-2.66; 0.20	5
b	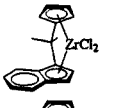	99.4	117.1	15.1; 12.6	71.6	85.7	2.45-2.63; 0.18	19
c	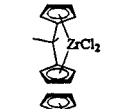	99.8	116.6	14.2	71.4	86.0	2.45-2.56; 0.12	20
d	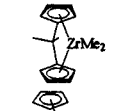	99.0	115.6	13.6	71.8	86.3	2.46-2.57; 0.11	21
e	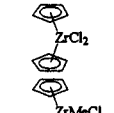		129.0		53.5	88.8	2.46-2.53; 0.07	22
f	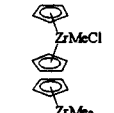		131.1		50.8	89.1	2.49-2.53; 0.04	23
g	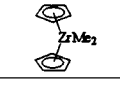		132.5		50.1	88.7	2.49-2.55; 0.06	23

Chart 3

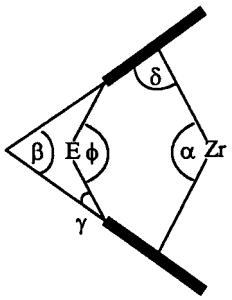

than in **5** and **2**, **2m**, and **b**−**d** (Δr = 0.11−0.20 Å). For unbridged molecules, Δr = 0.04−0.07 Å.

These differences are, likely, caused by the bulky ^{t}Bu substituents at C(3) of both indenyl fragments. This conclusion is supported by significant displacements of the C(3)−C^{t}Bu bonds from the planes of the parent cyclopentadienyl rings (10.0° and 8.2°) opposite to Zr. Moreover, the Zr−C(3) and Zr−C(3′) bond distances are among the longest.

The distinction between **4** and **5** are, apparently, associated with the different spatial location of the $SiMe_3$ and ^{t}Bu substituents. The C(3)−C_{tBu} bond distance (1.55 Å) is significantly shorter than the C(3)−Si distance (1.87 Å). Hence, the ^{t}Bu substituents are situated closer to the coordination sphere of the Zr atom than the $SiMe_3$ and affect its catalytic behavior more significantly. The displacement of the C(3)−Si bond in **5** (8.0°) is similar to that of the C(3)−C_{tBu} bond in **4**.

It should be noted that the X−Zr−X angle is little sensitive to the steric hindrance of the ligands. Little correlation is observed between this geometrical parameter and the type of geometry distortions for the groups of molecules selected in Table 1. This parameter varies within 98.7−100.8 (**4**, **5**, **2**, **2m**, and **b**−**d**), 96.8−99.3 (**a** and related Si-bridged complexes), and 95.5−97.1° (**e**−**g**).

3. Influence of Ligand Structure. In Table 2 we compare

Table 2. Propene Polymerization with Racemic Zirconocene/MAO Catalysts[a]

zirconocene	tacticity[b] b_{obsd}[d]	tacticity[b] % *mmmm*	total regioinversions (%)[c]	T_m (°C)	M_v[e]
$Me_2C(Ind)_2ZrCl_2$	0.958_0	80.6_9	0.3_8	127	11 100
$C_2H_4(Ind)_2ZrCl_2$[f]	0.973_7	87.4_7	0.5_5	134[f]	33 600[f]
$C_2H_4(4,7\text{-}Me_2\text{-}Ind)_2ZrCl_2$[f]	0.983_1	91.8_4	2.8_0[g]	131[f]	6 700[f]
$Me_2Si(Ind)_2ZrCl_2$	0.979_8	90.3_0	0.4_8	144	56 000
$Me_2Si(2\text{-}Me\text{-}Ind)_2ZrCl_2$	0.988_2	94.2_5	0.3_3	148	231 500
$C_2H_4(3\text{-}Me\text{-}Ind)_2ZrCl_2$	0.723_3	19.9_6	0	amorphous	15 800[h]
$Me_2C(3\text{-}^tBu\text{-}Ind)_2ZrCl_2$	0.989_4	94.8_0	0	152	88 700[f]
$Me_2C(3\text{-}SiMe_3\text{-}Ind)_2ZrCl_2$	0.973_3	87.3_6	0	138[f]	69 700[f]

[a] Polymerization conditions: 1 L stainless-steel autoclave, propene (0.4 L), 50 °C, 1 h, zirconocene/MAO aged 10 min. [b] Determined assuming the enantiomorphic site model, see ref 37. [c] Total regioirregular units (2,1 erythro + 2,1 threo + 3,1) determined as described in ref 37; end groups not included. [d] In liquid monomer, $b_{obsd} \rightarrow b$. [e] Determined from experimental intrinsic viscosity (THN, 135 °C) according to the $[\eta] = K(\bar{M}_v)^a$ with $K = 1.93 \times 10^{-4}$ and $\alpha = 0.74$.[48] [f] Average values. [g] End groups included. [h] Calculated from $[\eta]$ according to the $[\eta] = K(M_v)^a$ with $K = 1.85 \times 10^{-4}$ and $\alpha = 0.737$.[49]

the molecular characterization of iPP from a series of different zirconocenes in which the bridge length and indene substitution are varied. The type of bridge ($Me_2C<$, $-CH_2CH_2-$, $Me_2Si<$), in line with all previously reported results, is found to influence both the molecular weight of PP and its isotacticity, which both increase on going from $Me_2C<$ to $-CH_2CH_2-$ and then $Me_2Si<$. This effect is, however, limited, as molecular weights only increase from ca. 10^4 to ca. 5×10^4 on going from **2** to *rac*-$Me_2Si(Ind)_2ZrCl_2$ at 50 °C, with isotacticities increasing from 80 to 90%. On the other side, we found substitution at carbon 3 of the Cp ring of indene to have a stronger influence on catalyst performance. The size of the R group at C(3) determines both the degree of isotacticity and the molecular weight of PP, making this a highly versatile class of catalysts. In fact, molecular weights increase from 11 000 (**2**/MAO, R = H) to 88 000 (**4**/MAO, R = ^{t}Bu) while *mmmm* range from 80 to 95%. *This necessarily goes through a reversal of enantioface selectivity*.[24] In fact, $Me_2C(3\text{-}Me\text{-}Ind)_2ZrCl_2$ (2:1 rac/meso mixture; we were not able to isolate the pure rac isomer) produces a fully amorphous, low molecular weight polymer.

It is immediately apparent that, in terms of stereoselectivity, our novel catalyst **4**, with *mmmm* (50 °C) = 95% and T_m = 152 °C, compares favorably to all zirconocenes of Table 2, as well as representing a great improvement with respect to its Si-bridged analogue, *rac*-$Me_2Si(3\text{-}^tBu\text{-}Ind)_2ZrCl_2$.[8]

In general, isospecific zirconocenes produce iPP with incomplete regioselectivity that is allowing the insertion of occasional, isolated secondary (2,1 erythro and threo) units.[25]

We have previously shown that 2,1 units greatly reduce iPP molecular weight, because the rate of β-H transfer after a secondary insertion is higher than after a primary insertion, relative to monomer insertion.[16] In fact, *rac*-C_2H_4(4,7-dimethyl-1-indenyl)$_2ZrCl_2$/MAO, with about 3% 2,1 insertions, produces iPP with a 5-fold decrease in molecular weight than *rac*-C_2H_4(1-indenyl)$_2ZrCl_2$/MAO, which only allows for the formation of 0.6% regioirregularities (see Table 2).

While reinvestigating the polymerization behavior of **3**/MAO,[1a] we found this almost aspecific catalyst to be highly regiospecific.[26] The same behavior is retained by catalysts **4**/MAO and **5**/MAO, which in addition are isospecific and produce higher molecular weights than **1**−**3**.

Hence, all zirconocenes with *ansa*-bisindenyl ligands bearing alkyl groups on C(3) are *fully regiospecific*. The methyl region of the ^{13}C NMR spectra ($C_2D_2Cl_4$, 130 °C, 125 MHz) of PPs made with *rac*-[C_2H_4(4,7-dimethyl-1-indenyl)]$_2ZrCl_2$/MAO (A), **3**/MAO (B), and **4**/MAO (C) in liquid monomer at 70 °C, is shown in Figure 2.

It is apparent that, in contrast to iPP from *rac*-[C_2H_4(4,7-dimethyl-1-indenyl)]$_2ZrCl_2$/MAO, both PP samples B (atactic) and C (isotactic) show no peaks due to either 2,1 or 3,1 units.[25] In addition, while end groups due to both *cis*-2-butenyl (*cis*-$CH_3-CH{=}CH-CH_2P$, 12.9 ppm)[16] and *n*-propyl ($CH_3-CH_2-CH_2P$, 14.5 ppm) are clearly visible in sample A, samples B and C show only traces of the *n*-propyl end group, providing further evidence for the high regiospecificity of both **3**/MAO and **4**/MAO catalysts.

One of the rationales for designing ansa ligands with indenes bearing alkyl groups on C(3) was the hope that such a substitution pattern would suppress β-H transfer after primary insertion.[27j] However, end group analysis reveals that other transfer reactions, notably β-methyl elimination,[27] become available to **3**−**5**.

^1H NMR analysis of unsaturated end groups of low molecular weight polypropenes obtained from MAO-activated zirconocenes **1**−**5** and *rac*-$Me_2C(3\text{-}^tBu\text{-}4,5,6,7\text{-tetrahydro-1-indenyl})_2ZrCl_2$

(17) (a) Zaegel, F.; Galucci, J.; Meunier, P.; Gautheron, B.; Sivik, M. R.; Paquette, L. A. *J. Am. Chem. Soc.* **1994**, *116*, 6466. (b) Harder, S.; Prosenc, M. H. *Angew. Chem., Int. Ed. Engl.* **1994**, *33*, 1744. (c) Hong, J.-H.; Pan, Y.; Boudjouk, P. *Angew. Chem., Int. Ed. Engl.* **1996**, *35*, 186.

(18) Voskoboinikov, A. Z.; Agarkov, A. Yu.; Churakov, A. V.; Kuz'mina, L. G. *Izv. Akad. Nauk, Ser. Khim.* **1996**, *3*, 765.

(19) Green, M. L. H.; Ishihara, N. *J. Chem. Soc., Dalton Trans.* **1994**, 657.

(20) Shaltout, R. M.; Corey, J. Y.; Rath, N. P. *J. Organomet. Chem.* **1995**, *503*, 205.

(21) Nifant'ev, I. E.; Churakov, A. V.; Urazowski, I. F.; Mkoyan, Sh. G.; Atovmyan, L. O. *J. Organomet. Chem.* **1992**, *435*, 37.

(22) Prout, K.; Cameron, T. S.; Forder, R. A.; Critchley, S. R.; Denton, B.; Rees, G. V. *Acta Crystallogr.* **1974**, *B30*, 2290.

(23) Hunter, W. E.; Hrncir, D. C.; Bynum, R. V.; Penttila, R. A.; Atwood, J. L. *Organometallics* **1983**, *2*, 750.

(24) Toto, M.; Cavallo, L.; Corradini, P.; Moscardi, G.; Resconi, L.; Guerra, G. Submitted for publication.

(25) (a) Soga, K.; Shiono, T.; Takemura, S.; Kaminsky, W. *Makromol. Chem., Rapid Commun.* **1987**, *8*, 305. (b) Grassi, A.; Zambelli, A.; Resconi, L.; Albizzati, E.; Mazzocchi, R. *Macromolecules* **1988**, *21*, 617. (c) Grassi, A.; Ammendola, P.; Longo, P.; Albizzati, E.; Resconi, L.; Mazzocchi, R. *Gazz. Chim. It.* **1988**, *118*, 539. (d) Cheng, H.; Ewen, J. *Makromol. Chem.* **1989**, *190*, 1931. (e) Tsutsui, T.; Ishimaru, N.; Mizuno, A.; Toyota, A.; Kashiwa, N. *Polymer* **1989**, *30*, 1350. (f) Tsutsui, T.; Mizuno, A.; Kashiwa, N. *Makromol. Chem.* **1989**, *190*, 1177. (g) Tsutsui, T.; Kioka, M.; Toyota, A.; Kashiwa, N. In *Catalytic Olefin Polymerization, Studies in Surface Science and Catalysis;* Keii, T., Soga, K. Eds.; Elsevier: 1990; Vol. 56, p 493. (h) Rieger, B.; Chien, J. *Polymer Bull.* **1989**, *21*, 159. (i) Rieger, B.; Mu, X.; Mallin, D.; Rausch, M.; Chien, J. *Macromolecules* **1990**, *23*, 3559. (j) Chien, J.; Sugimoto, R. *J. Polym. Sci., Part A: Polym. Chem.* **1991**, *29*, 459. Mizuno, A.; Tsutsui, T.; Kashiwa, N. *Polymer* **1992**, *33*, 254. The correct nomenclature for these structures should be secondary meso and secondary racemic. We use here Zambelli's nomenclature,[24b] erythro (E) and threo (T) respectively, to avoid confusion with meso, rac dyad definition.

(26) Resconi, L.; Piemontesi, F.; Camurati, I.; Rychlicki, H.; Colonnesi, M.; Balboni, D. *Polym. Mater. Sci. Eng.* **1995**, *73*, 516.

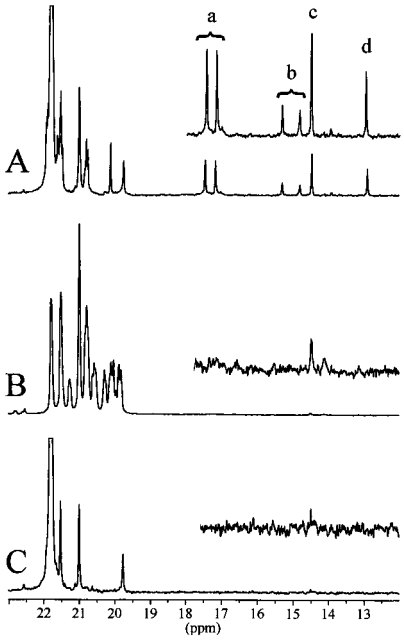

Figure 2. ^{13}C NMR methyl region of iPP samples (liquid propene polymerizations at T_p = 70 °C) from *rac*-[C_2H_4(4,7-dimethyl-1-indenyl)]$_2ZrCl_2$/MAO (A), **3**/MAO (B), and **4**/MAO (C): (*a*) 2,1 erythro; (*b*) 2,1 threo; (c) −CH(CH_3)$CH_2CH_2CH_3$; (d) *cis*-CH(CH_3)CH_2-CH=CHCH_3.

(**4**-H_4),[28] in liquid propene at 70 °C, are shown in Table 3. The end group structure of iPP from **1** has been already presented[16] and is discussed here in more detail.

The olefin region of the ^{1}H NMR spectra ($C_2D_2Cl_4$, 120 °C, 400 MHz) of the above PP samples are shown in Figure 3.

iPP from **1**/MAO shows *four* olefinic end groups: *cis*-2-butenyl (5.4−5.55 ppm, 39.1%,), a triplet at 5.21 ppm (17.4%), the two vinylidene peaks (4.7−4.8 ppm, 29.5%) and a fourth, previously unreported peak overlapping the lowest field vinylidene peak (13.9%). The triplet at 5.21 ppm has been tentatively assigned to the isobutenyl group formed by isomerization of the terminal vinylidene.[7b] We reassigne it to the vinylic proton in the $CH_3CH_2CH_2CH$=C(CH_3)CH_2P structure.[29]

The situation for iPP from **2**/MAO is simpler: possibly due to its larger "bite angle" (β = 70.9° versus 60.4 in **1**, see Table 1), **2** favors β-H elimination after primary insertion (about 80% vinylidene end groups), producing iPP with lower molecular weight and lower isotacticity than **1**. The marginally isospecific **3**/MAO at 50 °C in liquid monomer produces amorphous polypropene with molecular weights intermediate between those of **1** and **2**. Compound **3** (which is fully regiospecific, and hence, devoid of the possibility of forming *cis*-2-butenyl end groups) allows chain transfer to occur via both β-hydrogen transfer after a primary insertion (vinylidene, 69%) and, already in liquid monomer, unimolecular β-methyl transfer (allyl, 31%). The presence of β-methyl transfer in **3** was expected as zirconocenes with peralkylated cyclopentadienyl ligands were shown to have the same behavior.[27] Catalyst **4**/MAO shows the highest selectivity for β-methyl transfer (43.2% of allyl groups) so far observed in an isospecific zirconocene.

A complete stereochemical and mechanistic analysis of end group formation in propene polymerization with **1**−**4** will be reported in the future. Here, we note that **4**/MAO at 70 °C produces iPP with a relevant amount of isobutenyl (Me_2C=C*H*−CHMe−, doublet at 4.9 ppm, 30%) end groups, which *does not* arise from acidic isomerization of the vinylidene end group, but must be the product of a new chain transfer reaction. To further support this hypothesis, we have prepared the hydrogenated version of **4**, *rac*-Me_2C(3-^{t}Bu-4,5,6,7-tetrahydro-1-indenyl)$_2ZrCl_2$ (**4**-H_4), which has a bulkier ligand. As a matter of fact, **4**-H_4/MAO is less active, less stereospecific, and makes lower molecular weight PP than **4**/MAO.[28] End group analysis shows a much higher content of the isobutenyl end group (46.6% vs 30.4%) and a much lower content of the allyl end group (7.8 vs 43.2%) in iPP from **4**-H_4 compared to iPP from **4**.

The presence of the isobutenyl end group could be seen as supporting evidence for Busico's and Brintzinger's hypothesis of a Cp′$_2$Zr$^+$−C(Me)$_2$P (*P* = polypropene growing chain) as the key intermediate for epimerization[30] and primary, unimolecular β-H transfer.[31] For our catalyst **4**, with β-H transfer inhibited by the steric hindrance of the 3-*tert*-butyl indenyl ligands, on one side β-methyl transfer becomes competitive; on the other, the same conformation leading to β-methyl transfer might facilitate the formation of the tertiary alkyl intermediate. This, in turn, can generate a number of (likely unimolecular) reactions: epimerization, β-H transfer from either one of the two *gem*-methyl groups, or the novel β-H transfer from the β-methylene.[32]

A second, important feature of the unsaturated groups is that, almost invariably, the two terminal vinylidene peaks do not have the same intensity, with the lower field peak being the more intense. This means that an additional, symmetric vinylidene group is present in iPPs made with *C_2-symmetric* zirconocenes, a group so far gone unnoticed. This vinylidene species has the same chemical shift as the vinylidene in 4-methyl-1-pentene oligomers, and we tentatively assign it to a species of structure ^{i}Bu-C(=CH_2)CH_2CH(CH_3)CH_2P. This peak is never observed in atactic PP produced with C_{2v}-symmetric zirconocenes. For iPP from **4**/MAO, this internal vinylidene (15.5%) is more frequent than the normal vinylidene (10.9%), and for **5** it is by far the most intense one (62.7%). Comparing the ^{1}H NMR spectra of the olefin region of iPP samples from **1**−**5**, we conclude that this internal vinylidene competes with β-Me elimination, which might indicate that its formation requires a crowded environment but less so than the one required for β-Me elimination.[33−35] It is worth noting that, in the more crowded

(27) A now large number of highly substituted ligands have been found to trigger β-Me transfer. (a) Eshuis, J.; Tan, Y.; Teuben, J. H.; Renkema, J. *J. Mol. Catal.* **1990**, *62*, 277. (b) Eshuis, J.; Tan, Y.; Meetsma, A.; Teuben, J. H. *Organometallics* **1992**, *11*, 362. (c) Resconi, L.; Piemontesi, F.; Franciscono, G.; Abis, L.; Fiorani, T. *J. Am. Chem. Soc.* **1992**, *114*, 1025. (d) Yang, X.; Stern, C. L.; Marks, T. J. *Angew. Chem., Int. Ed. Engl.* **1992**, *31*, 1375. (e) Mise, T.; Kageyama, A.; Miya, S.; Yamazaki, H. *Chem. Lett.* **1991**, 1525. (f) Kesti, M.; Waymouth, R. *J. Am. Chem. Soc.* **1992**, *114*, 3565. (g) Guo, Z.; Swenson, D.; Jordan, R. *Organometallics* **1994**, *13*, 1424. (h) Hajela, S.; Bercaw, J. E. *Organometallics* **1994**, *13*, 1147. (i) Yang, X.; Stern, C. L.; Marks, T. J. *J. Am. Chem. Soc.* **1994**, *116*, 10015. (j) Resconi, L.; Jones, Rheingold, A.; Yap, G. P. A. *Organometallics* **1996**, *15*, 998.

(28) *rac*-Me_2C(3-^{t}Bu-H_4-Ind)$_2ZrCl_2$ (**4**-H_4)was synthesized by catalytic hydrogenation of parent **4** (see the Experimental Section). **4**-H_4/MAO polymerizes propene (liquid monomer, 70 °C, Al/Zr = 3000, Zr = 1.81 mmol) with low activity (10 000 g_{PP}/(mmol$_{Zr}$ h)) to iPP with both low molecular weight (see Table 3) and low isotacticity.

(29) The triplet at 5.2 ppm arises from coupling of a vinylic proton with a neighboring methylene (J_{H-H} = 7 Hz). This peak is observed *only* in conjunction with the *cis*-2-butenyl end group; therefore, it must be connected to the presence of secondary insertions. We exclude that its formation is due to acid-catalyzed isomerization of a 2-butenyl unit during polymer workup or NMR analysis, as the *cis*-2-butenyl group is fully stable in the presence of added acids (*p*-toluenesulfonic acid, $C_2D_2Cl_4$, 130 °C, 30′). The assignment of the triplet at 5.2 ppm to the proposed structure CH_3-CH_2CH_2CH=C(CH_3)−CH_2P is supported by acidic isomerization, which in part generates the *cis*-/*trans*-$CH_3CH_2CH_2CH_2$C(CH_3)=C*H*P group. Other experiments are underway to confirm this assignment.

(30) Busico, V.; Cipullo, R. *J. Am. Chem. Soc.* **1994**, *116*, 9329.

(31) Leclerc, M.; Brintzinger, H.-H. *J. Am. Chem. Soc.* **1995**, *117*, 1651.

(32) Schneider, M. J.; Mülhaupt, R. *Macromol. Chem. Phys.* **1997**, *198*, 1121.

Table 3. Olefin End Groups Distributions for iPP Samples from **1**−**5**[a]

Catalyst	% of total unsaturated end groups [b]					$\bar{P}_n$ [b]	frequency of chain transfer		
	a	b	d	e	f		primary β-H	β-Me	secondary β-H
1 [c]	29.5	13.9	-	-	39.1	384	1.1×10^{-3}	-	1.5×10^{-3}
2	69.0	10.5	-	-	20.5	134	5.9×10^{-3}	-	1.5×10^{-3}
3	39.2	9.1	-	51.7	-	221	2.2×10^{-3}	2.3×10^{-3}	-
4	10.9	15.5	30.4	43.2	-	327	1.7×10^{-3}	1.3×10^{-3}	-
4-H$_4$	45.6	-	46.6	7.8	-	14	6.7×10^{-2}	5.6×10^{-3}	-
5	21.6	62.7	3.8	11.9	-	283	3.1×10^{-3}	4.2×10^{-4}	-

[a] Liquid monomer, $T_p = 70$ °C. See following tables for polymerization details. [b] From ^{1}H NMR, 400 MHz. $\bar{P}_n$ is evaluated assuming one double bond per chain. [c] Triplet at 5.2 accounts for 17.4% and is included in the frequency of secondary transfer.

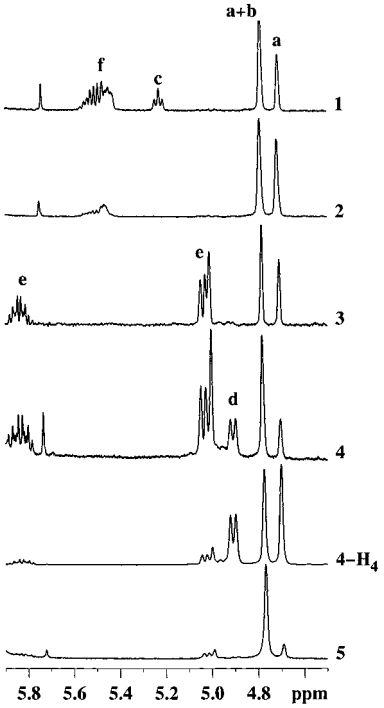

Figure 3. ^{1}H NMR olefin region of low molecular weight iPP samples (liquid propene polymerizations at $T_p = 70$ °C) from **1**−**5**/MAO: (a) vinylidene, (b) internal vinylidene, (c) $CH_3CH_2CH_2CH{=}C(CH_3)P$, (d) isobutenyl, (e) allyl, (*f*) 2-butenyl.

system **4**-H$_4$, the internal vinylidene is not formed, and the allyl group is reduced to only 7.8%, despite the very low molecular weight ($\bar{P}_n = 14$).

Hence, **4** and **5** produce higher molecular weights than **1** and **2** because of their much higher regiospecificity and, possibly, reduced rate of β-H transfer after primary insertion. Unfortunately, despite their high regiospecificity, **4** and **5** fail to produce iPP with high enough molecular weights to cover all industrially produced iPP grades. However, their easy synthetic accessibility, and the fact that their meso isomers are *inactive* toward propene homopolymerization (vide infra), makes them potential candidates for the production of the lowest molecular weight grades. The lower than desired molecular weights are due to the onset of β-Me elimination, *already in liquid monomer*, for **4**, and to the newly identified chain transfer reaction, forming the internal vinylidene group, for **5**.

At this point in time, it seems that substitution at the 2 position of indene,[5−7] effectively reducing chain transfer to the monomer after both primary and secondary insertions,[7,36] remains the most successful strategy to increase iPP molecular weight.

4. Influence of the Polymerization Temperature. The second most important source of variability in the molecular architecture of polypropenes obtained from *ansa*-zirconocenes, in addition to the biscyclopentadienyl ligand structure, are the polymerization conditions.[1] The influence of polymerization

(33) Concerning the mechanism of its formation, a possible hypothesis is based on intramolecular σ-bond metathesis[34] (sp^3 C−H activation[35] involving insertion of a methyl C−H bond of the penultimate unit into the Zr−C bond, followed by β-H elimination). This mechanism requires very little atomic motion and is essentially the same already proposed by us to explain the formation of linear propylene tetramers in the dimerization of 4-methyl-1-pentene by Cp*$_2$HfCl$_2$/MAO (Cp* = pentamethylcyclopentadienyl):[27c]

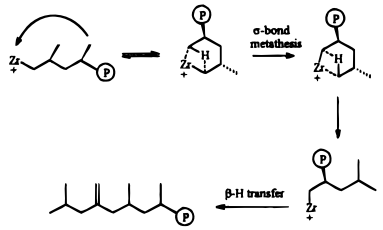

Alternatively, the internal vinylidene could arise from reinsertion of an allyl-terminated iPP chain, followed by β-H transfer. We are currently testing these two hypotheses.

(34) The mechanism and scope of σ-bond metathesis at permethylscandocene derivatives has been described by Bercaw and extended to methyl zirconocene cations by Jordan: Thompson, M.; Baxter, S.; Bulls, A.; Burger, B.; Nolan, M.; Santarsiero, B.; Schaefer, W.; Bercaw, J. *J. Am. Chem. Soc.* **1987**, *109*, 203 and references therein. Jordan, R.; Taylor, D.; Baenziger, N. *Organometallics* **1990**, *9*, 1546.

(35) Although most *intramolecular* C−H activation reactions involve the formation of a metal−hydrogen bond (such as β-hydride transfers), *intermolecular* C−H activation at early transition metals invariably leads to the formation of metal−carbon bonds:

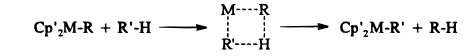

See also: Watson, P.; Parshall, G. *Acc. Chem. Res* **1985**, *18*, 51 and references therein. Intramolecular sp^3 C−H activation in early transition metal complexes bearing alkyl groups long enough to make both interactions geometrically accessible, creates a Zr−C bond: for example, the reaction of (^{t}Bu$_2$Cp)$_2$ZrMe$_2$ with B(C$_6$F$_5$)$_3$ was shown by Marks (Yang, X.; Stern, C.; Marks, T. *J. Am. Chem. Soc.* **1994**, *116*, 10015) to generate a CpCMe$_2$-CH$_2$Zr metallacycle and CH$_4$, via σ-bond metathesis.

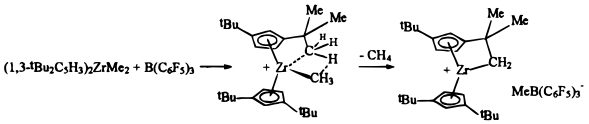

See also: Rothwell, I. P. *Acc. Chem. Res* **1988**, *21*, 153 and Ryabov, A. D. *Chem. Rev.* **1990**, *90*, 403 and references therein.

(36) Cavallo, L.; Guerra, G. *Macromolecules* **1996**, *29*, 2729.

Table 4. Propene Polymerization with **1**/MAO in Liquid Monomer at Different Temperatures[a]

sample no.	T_p (°C)	activity (g_{PP}/mmol$_{Zr}$ h)	$\bar{M}_v$ (dL/g)[b]	T_m (°C)	b_{obsd}[c]	*mmmm* (%)[c]	total regioirr (%)[d]
1	70	251 700	19 600	125	0.964_5	83.4_7	0.7_3
2	60	136 400	25 300	131	0.966_5	84.3_4	0.6_1
3	50	139 600	34 500	134	0.973_2	87.3_0	0.5_7
4	40	58 000	37 700	137	0.976_9	88.9_7	0.4_9
5	30	35 600	45 500	140	0.980_5	90.6_2	0.4_3
6	20	18 200	56 000	142	0.983_3	91.9_2	0.3_8

[a] Experimental conditions: catalyst/cocatalyst dissolved in 10 mL of hexane, aged 10 min; Zr = 0.48 μmol, M-MAO cocatalyst, 1.65 M (as Al) solution in isopar-C; Al/Zr = 8000; 1 h. [b] Determined from experimental intrinsic viscosities in THN at 135 °C from the $[\eta] = K(\bar{M}_v)^a$ with $K = 1.93 \times 10^{-4}$ and $\alpha = 0.74$.[48] [c] From ^{13}C NMR (125 MHz); determined assuming the enantiomorphic site model.[37] [d] Total regioirregularities (2,1 erythro + 2,1 threo + 3,1) determined according to ref 37.

Table 5. Propene Polymerization with **2**/MAO in Liquid Monomer at Different Temperatures[a]

sample no.	Zr (μmol)	T_p (°C)	activity (g_{PP}/mmol$_{Zr}$ h)	$\bar{M}_n$[b]	T_m (°C)	b_{obsd}[c]	*mmmm* (%)[c]	total regioirr (%)[d]
7	0.23	70	145 100	5 600	124	0.948_5	76.7_5	0.6_0
8	0.46	60	125 700	6 200	124	0.955_9	79.8_1	0.4_8
9	2.31	50	65 800	6 500	127	0.958_0	80.6_9	0.3_8
10	0.46	40	50 000	7 200	136	0.966_4	84.2_7	0.3_9
11	0.46	20	10 200	9 700	139	0.975_4	88.2_9	0.3_0
12	0.46	0	890	11 000	144	0.980_7	90.7_0	0.1_4

[a] Experimental conditions: catalyst/cocatalyst dissolved in 10 mL of hexane, aged 10 min; Al/Zr = 8000; MAO cocatalyst. 1 h. [b] Determined by ^{1}H NMR from the olefinic end group (80% vinylidene, 20% *cis*-2-butenyl), assuming one double bond per chain. The intrinsic viscosities in THN at 135 °C were too low to give reliable viscosity average molecular weights. [c] From ^{13}C NMR (125 MHz); determined assuming the enantiomorphic site model.[37] [d] Total regioirregularities (2,1 erythro + 2,1 threo; no 3,1 units were detected in these samples) determined according to ref 37.

conditions in particular is much more important than for the Ti-based heterogeneous catalysts.

We[37] and others[30,31,38] have recently shown that the stereoregularity, regioregularity, and molecular weight of isotactic polypropenes from *C_2-symmetric* zirconocenes can be highly dependent on monomer concentration: by decreasing [propene], polypropenes with decreasing molecular weights and isotacticity, and varying regioregularities, are obtained.

Polymerization temperature (T_p) is another parameter with a major influence on PP characteristics, but most of the previous studies have been carried out in solution at largely different propene concentrations, so changes in the latter due to lower propene concentrations at the higher T_p become the primary cause for changes on both polymer properties and polymerization kinetics, rather than T_p itself.

It is therefore of the utmost importance, when comparing the polymerization performance of different zirconocene catalysts, to perform the experiments under high and identical monomer concentrations, and preferably in liquid propene, to minimize the extent of chain end epimerization. We have already reported the results of our investigation on the effect of polymerization temperature, in *liquid monomer* in the temperature range of 20−70 °C, on the polymerization kinetics and the structural details of iPP produced with the two *C_2-symmetric* zirconocene catalysts **1**/MAO and **3**/MAO.[26]

Here we report the influence of T_p, in *liquid monomer*, on the structural details of iPP produced with **4**/MAO and **5**/MAO, compared to **1**−**3**.

Propene Polymerization Performance of 1/MAO. As previously observed by a number of other authors,[1] both isotacticity and molecular weight of iPP from **1**/MAO decrease by increasing T_p, while the amount of secondary insertions increases slightly. The stereospecificity of *C_2-symmetric* zirconocenes is also adversely affected by decreasing propene concentration, due to the onset of the parasitical growing-chain-end epimerization reaction.[30,38b,c] The rate of epimerization is a function of both the polymerization temperature and the ligand structure.

In liquid monomer, however, epimerization is not observed, at least in the T_p range investigated by us. The relevant polymerization results from **1**/MAO are summarized in Table 4. The microstructure of iPP samples from **1**/MAO reported in ref 2 have been reanalyzed by means of a 500 MHz spectrometer (see Table 4), which provided results very similar to the previous ones (300 MHz). The apparent Bernoullian stereospecificity parameter b_{obsd} and the relative amounts of the three different types of secondary units have been determined as previously described.[37] The better evaluation of the smaller signals, obtained with a higher field, allowed us to obtain more reliable energy values (vide infra).

In our polymerization conditions, increasing T_p from 20 to 70 °C, **1**/MAO yields polypropenes with $\bar{M}_v$ values ranging from 56 000 to 19 600, percent *mmmm* pentads from 92 to 83%, and corresponding melting temperatures from 142 to 125 °C. Furthermore, the overall fraction of regioirregularities (2,1 and 3,1 insertions) increases from 0.4 to 0.7%.

Propene Polymerization Performance of 2/MAO. Compound **2** was tested to measure the effect of a wider "bite angle" β (see Table 1) on catalyst performance, in the absence of added substituents. The relevant polymerization results are reported in Table 5. **2**/MAO is slightly less isospecific than **1**/MAO as percent *mmmm* pentads decrease from 88 to 77% by increasing T_p from 20 to 70 °C. The regiospecificity of **2** is slightly higher (percent 2,1 insertions from 0.1_4 at 0 °C to 0.6_0 % at 70 °C) than that of **1**. These findings are in agreement with, and explained by, the mechanistic model proposed by Guerra, which

(37) Resconi, L.; Fait, A.; Piemontesi, F.; Colonnesi, M.; Rychlicki, H.; Zeigler, R. *Macromolecules* **1995**, *28*, 6667.

(38) (a) Rieger, B.; Jany, G.; Fawzi, R.; Steimann, M. *Organometallics* **1994**, *13*, 647. (b) Busico, V.; Cipullo, R.; Chadwick, J. C.; Modder, J. F.; Sudmeijer, O. *Macromolecules* **1994**, *27*, 7538. (c) Leclerc, M.; Brintzinger, H.-H. *J. Am. Chem. Soc.* **1996**, *118*, 9024.

Table 6. Propene Polymerization with **3**/MAO in Liquid Monomer at Different Temperatures[a]

sample no.	Zr (μmol)	Tp (°C)	activity ($g_{PP}/mmol_{Zr}$ h)	$\bar{M}_w$ (g/mol)[b]
13	0.45	70	81 300	11 300
14	0.45	50	28 400	15 800
15	1.12	35	10 100	29 000
16	1.12	20	2 800	36 900
17	8.96	0	850	54 200

[a] Experimental conditions: catalyst/cocatalyst dissolved in 10 mL of hexane, aged 10 min; Al/Zr = 8000; 1 h. All samples are amorphous. [b] Calculated from experimental intrinsic viscosities (THN, 135 °C) according to the $[\eta] = K(\bar{M}_w)^a$ with $K = 1.85 \times 10^{-4}$ and $a = 0.737$.[49]

Table 7. ^{13}C NMR Characterization of iPP Samples Prepared with **3**/MAO

		exptl triad distrib. (%)					tacticity[a]	
sample	T_p (°C)	*mm*	*rm*	*rr*	B^b	E^c	b_{obsd}	*mmmm*
13	70	32.1_0	43.1_2	24.7_8	1.7_1	1.1_5	0.672_7	14.1_5
14	50	39.0_9	39.8_3	21.0_8	2.0_8	1.0_6	0.723_3	19.9_6
15	35	44.4_8	37.1_2	18.4_0	2.3_8	0.9_9	0.750_2	23.8_6
16	20	46.0_2	34.8_6	19.1_2	2.9_0	1.1_0	0.762_6	25.8_7
17	0	55.5_8	30.2_9	14.1_3	3.4_2	0.9_3	0.813_7	35.6_9

[a] Determined assuming the enantiomorphic site model.[37] No secondary units could be detected (^{13}C NMR, 125 MHz). [b] Bernoullian triad test, $B = 4[mm][rr]/[mr]^2$. $B = 1$ for perfect chain end control. [c] Enantiomorphic site triad test, $E = 2[mm]/[mr]$. $E = 1$ for perfect site control.

connects regiospecificity and stereospecificity in propene polymerization with *C_2-symmetric* metallocenes.[39]

It is worth noting here that there is no detectable 2,1 → 3,1 isomerization with **2**/MAO, as only 2,1 erythro and 2,1 threo units were observed. As the 2,1 → 3,1 isomerization reaction would be faster than epimerization, its absence (or very low extent, as in **1**/MAO[26]) is an indication of the absence of epimerization in liquid monomer.

Molecular weights of iPP from **2**/MAO are lower than those obtained from **1**/MAO at any temperature in the range investigated, ranging (assuming $\bar{M}_w/\bar{M}_n \approx 2$) from $\bar{M}_v \approx 20\,000$ ($\bar{M}_n = 11\,000$ at $T_p = 0$ °C) to $\bar{M}_v \approx 12\,000$ ($\bar{M}_n = 6000$ at $T_p = 70$ °C). It is also interesting that the temperature dependence of molecular weights of iPP from **2**/MAO is lower than that shown by **1**/MAO (see below).

Propene Polymerization Performance of 3/MAO. Ewen has reported that *rac*-[ethylenebis(3-methyl-1-indenyl)]$ZrCl_2$/methylalumoxane catalyst (**3**/MAO) is nearly aspecific despite its C_2-symmetry.[1a] We have reinvestigated the behavior of **3**/MAO in liquid monomer and confirmed that it is far less isospecific than **1**/MAO: percent *mmmm* pentads decrease from 36 to 14% ($b_{50\,°C} = 0.723_3$) with an increase in T_p from 0 to 70 °C.[26] The relevant polymerization results are reported in Tables 6 and 7.

The polymerization mechanism is not immediately obvious by looking at the pentad region of the ^{13}C NMR, due to the presence of all pentads. Application of the statistical triad tests allows to identify the source of the weak enantioface selectivity in **3**/MAO as being enantiomorfic site control, as it is the case of all other *C_2-symmetric* systems investigated here.

This is only possible by looking at the T_p dependence of the *E* and *B* parameters: only the correct mechanism shows invariance with T_p of the corresponding triad test (Table 7).

Close inspection of the ^{13}C NMR (125 MHz) of sample 13 ($T_p = 70$ °C) shows that, interestingly, **3** is *fully regiospecific*: no regiomistakes of any kind could be detected. The amorphous polypropenes produced with **3**/MAO also have molecular weights lower than those from **1**/MAO. The fact that **3** gives lower molecular weights than **1** appears to be a direct consequence of the lower activity (lower rate of propagation) of the former and not of a higher chain transfer rate. Actually, due to the increased steric bulk of the ethylenebis(3-methyl-1-indenyl) ligand with respect to the ethylenebis(1-indenyl) ligand, we expect the overall rate of transfer to be lower in **3** than in **1** (see below).

Table 8. Propene Polymerization with **4**/MAO in Liquid Monomer at Different Temperatures[a]

sample no.	Zr (μmol)	T_p (°C)	activity ($g_{PP}/mmol_{Zr}$ h)	$\bar{M}_v$ (g/mol)[b]	T_m (°C)	b_{obsd} (%)[c]	*mmmm* (%)[c]
18	0.18	70	110 000	25 300	142	0.981_9	91.2_5
19	0.37	60	160 600	65 400	148	0.985_7	93.0_6
20	0.18	50	124 600	89 400	152	0.989_4	94.8_0
21	0.37	40	112 400	130 800	156	0.991_8[d]	95.5_2[d]
22	0.37	30	68 800	210 100	157	0.993_5	96.7_8
23	0.37	20	32 000	410 400	158	0.993_7	96.8_9

[a] Experimental conditions: catalyst/cocatalyst dissolved in 10 mL of toluene, aged 10 min; Al/Zr = 8000; MAO cocatalyst, 1 h. [b] Calculated from the experimental intrinsic viscosities ($[\eta]_{THN,\,135\,°C}$) according to the $[\eta] = K(\bar{M}_v)^a$ with $K = 1.93 \times 10^{-4}$ and $\alpha = 0.74$.[48] [c] Determined assuming the enantiomorphic site model.[37] No secondary units could be detected by ^{13}C NMR (125 MHz). [d] Average of two measurements.

Propene Polymerization Performance of 4/MAO. Building on the fact that **3** is highly regiospecific, and taking advantage of the easy synthetic accessibility of isopropylidene-bridged bisindenyl ligands, we selected the *rac*-[Me_2C(3-*tert*-butyl-1-indenyl)$_2$]$ZrCl_2$/MAO catalyst as the best possible candidate for an improved isospecific zirconocene catalyst. We found that **4**/MAO is a novel example of an isospecific zirconocene which is at the same time fully regiospecific and produces iPP with molecular weights much higher than those obtained with **1**−**3**, especially at the lowest T_p. Average viscosity molecular weights range from 410 000 at 20 °C to 25 000 at 70 °C (Table 8).

In addition, although its meso isomer is obtained in the reaction mixture and is difficult to separate from **4**, we found that rac/meso mixtures produce the same iPP as the pure racemic isomer, and indeed no atactic PP could be observed or extracted (all samples had no xylene-soluble fraction at room temperature). This was confirmed by a test in which the pure *meso*-[Me_2C-(3-*tert*-butyl-1-indenyl)$_2$]$ZrCl_2$/MAO catalyst was used and no polymer could be isolated, clearly showing that the meso isomer of **4** is inactive, at least in propylene homopolymerization, removing the need for a tedious zirconocene fractionation.

4/MAO, with percent *mmmm* always above 90%, is remarkably stereospecific. It is worth noting that this behavior is not only a feature related to the bulky ^{t}Bu group on C(3) but is also due to the single C bridge, which imparts to the molecule a high rigidity and a large bite angle ($\beta = 75.2°$, the largest of all zirconocenes shown in Table 1).

If any of these features are missing, a decrease in catalyst performance is observed. In fact, neither a silicon bridge nor an ethylene bridge produces good catalysts, as observed for *rac*-Me_2Si(3-^{t}Bu-Ind)$_2ZrCl_2$[8] and *rac*-C_2H_4(3-TMS-Ind)$_2ZrCl_2$.[40]

The melting points of iPP from **4**/MAO (142−158 °C) reflect their relatively high isotacticities.

Propene Polymerization Performance of 5/MAO. Despite their structural similarity, **5** has a notably lower performance

(39) Guerra, G.; Longo, P.; Cavallo, L.; Corradini, P.; Resconi, L. *J. Am. Chem. Soc.* **1997**, *119*, 4394.

(40) Spaleck, W.; Antberg, M.; Aulbach, M.; Bachmann, B.; Dolle, V.; Haftka, S.; Küber, F.; Rohrmann, J.; Winter In *Ziegler Catalysts*; Fink, G., Mülhaupt, R., Brintzinger, H.-H., Eds.; Springer-Verlag: Berlin, 1995; p 83.

Table 9. Propene Polymerization with **5**/MAO in Liquid Monomer at Different Temperatures[a]

sample no.	Zr (μmol)	T_p (°C)	activity (g_{PP}/mmol$_{Zr}$ h)	$\bar{M}_v$ (g/mol)[b]	T_m (°C)	b_{obsd}[c]	*mmmm* (%)[c]
24	0.52	70	43 600	44 300	127	0.958_0	80.6_8
25	0.52	60	59 400	65 800	130	0.964_3	83.3_7
26	0.87	50	73 600	70 900	135	0.970_1	85.9_1
27	6.93	40	14 200	73 500	139	0.971_0	86.3_2
28	0.87	30	39 000	121 900	145	0.975_1	88.1_6
29	6.93	20	9 600	120 400	146	0.978_1	89.5_2

[a] Experimental conditions: catalyst/cocatalyst dissolved in 10 mL of toluene, aged 10 min; MAO cocatalyst, Al/Zr = 3000; 1 h. [b] Calculated from the experimental intrinsic viscosities ($[\eta]_{THN,\ 135\ °C}$) according to the $[\eta] = K(\bar{M}_v)^a$ with $K = 1.93 \times 10^{-4}$ and $\alpha = 0.74$.[48] [c] Determined assuming the enantiomorphic site model.[37] No secondary units could be detected by ^{13}C NMR (125 MHz).

than **4**. In fact, isospecificity is negatively affected by substituting $SiMe_3$ for *tert*-butyl, and, in terms of stereoselectivity, **5**/MAO behaves quite like **1**/MAO. In terms of molecular weights, **5**/MAO produces iPP with notably higher molecular weights than **1**−**3** (Table 9). In comparison to **4**, **5** shows a lower temperature dependence: indeed, while **5**/MAO produces lower molecular weights than **4**/MAO at the lower temperatures, iPP molecular weights from **5**/MAO becomes slightly higher than those from **4**/MAO at 60−70 °C.

Discussion

Activity. The plot of ln(*A*/[M]) versus $1/T_p$ gives the apparent activation energy $\Delta E^{\ddagger}$ of the polymerization process.

The ln(*A*/[M]) versus $1/T_p$ plots for **1**−**3** gave values of 11.4 ± 0.9, 13.9 ± 1.1, and 15.0 ± 1.4 kcal/mol, respectively. For **4** and **5** we could not obtain a linear correlation in all T_p range due to reactor fouling and, possibly, partial catalyst deactivation at the higher temperatures.

The value of $\Delta E^{\ddagger}$ = 11.4 kcal/mol found for **1**/MAO is similar to the reported activation energy for propene polymerization with heterogeneous catalysts,[41] which is in the range of 10−13 kcal/mol and higher than that (7.6 kcal/mol) obtained by Kaminsky for **1**/MAO under nonconstant monomer concentration conditions.[42] There is no apparent correlation between catalyst activity and the steric bulk of the 3-R-1-indenyl ligand, as **4**/MAO (R = ^{t}Bu) is more active than **3**/MAO (R = Me). We do not attach any particular relevance to polymerization activities, these being affected by too many parameters. For example, a high apparent $\Delta E^{\ddagger}$ might be the result of the concentration of active sites increasing by increasing T_p.

Molecular Weight. On the contrary, molecular weight measurements are far less sensitive on random factors such as catalyst amount, catalyst/monomer purity, Al/Zr ratios (above a threshold), and, more important, on the number of active centers, but are highly sensitive on the catalyst structure, monomer concentration, and polymerization temperature.

Hence, reliable molecular weights can give much information on the nature of the active sites. The ln(P_n) versus $1/T_p$ plots give the overall activation energy barrier for chain transfer. The $\Delta\Delta E^{\ddagger}_{tr}$ for **1**−**5** are reported in Table 10, and the ln(P_n) versus $1/T_p$ plots for **2**, **4**, and **5** are shown in Figure 4. The higher energy barrier to transfer measured for **4**/MAO (10.7 kcal/mol) and the lower ones obtained for catalysts **1**/MAO (3.9), **2**/MAO (1.9), **3**/MAO (4.1), and **5**/MAO (4.1) can be, in first approximation, attributed to the higher conformational freedom of the growing chain in **1**−**3** versus the bulkier and more rigid catalyst **4** and the longer, more flexible C(3)−Si bond in **5**.

Table 10. Summary of Kinetic Data for **1**−**5**

zirconocene	$\Delta\Delta E^{\ddagger}_{enant}$ (kcal/mol)	$\Delta\Delta E^{\ddagger}_{tr}$ (kcal/mol)
$C_2H_4(Ind)_2ZrCl_2$	3.3 ± 0.2	3.9 ± 0.4
$Me_2C(Ind)_2ZrCl_2$	2.8 ± 0.2	1.9 ± 0.1
$C_2H_4(3\text{-Me-Ind})_2ZrCl_2$	1.9 ± 0.2	4.1 ± 0.8
$Me_2C(3\text{-}^t\text{Bu-Ind})_2ZrCl_2$	4.6 ± 0.6	10.7 ± 0.4
$Me_2C(3\text{-}Me_3Si\text{−Ind})_2ZrCl_2$	2.6 ± 0.2	4.1 ± 0.3

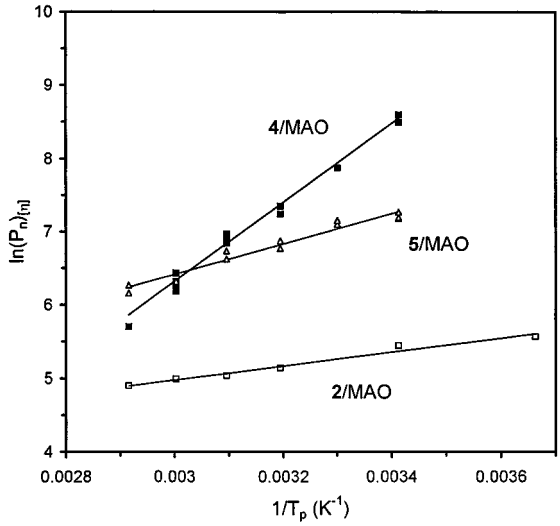

Figure 4. Arrhenius plot of ln($\bar{P}_n$) versus $1/T_p$ for **2**, **4**, and **5**: (□) **2**/MAO, $\Delta\Delta E^{\ddagger}$ = 1.9 ± 0.1 kcal/mol, R = 0.988; (■) **4**/MAO, $\Delta\Delta E^{\ddagger}$ = 10.7 ± 0.4 kcal/mol, R = 0.992; (Δ) **5**/MAO, $\Delta\Delta E^{\ddagger}$ = 4.1 ± 0.3 kcal/mol, R = 0.979. $\bar{P}_n$ is the number average degree of polymerization as estimated from average viscosity molecular weights, assuming $\bar{M}_v = \bar{M}_w$ and $\bar{M}_w/\bar{M}_n = 2$ (catalysts **4**/MAO and **5**/MAO, see Tables 8 and 9), or from ^1H NMR, assuming one double bond per chain (catalyst **2**/MAO, see Table 5).

Stereoregularity. The isospecificity of a catalyst is defined by the statistical parameter *b*, which represents the probability of a "correct" monomer insertion in the enantiomorphic site, at a given polymerization temperature. Under our experimental conditions (i.e., in liquid monomer), we assume epimerization to be negligible; hence, the measured values of the parameter b_{obsd} can be assumed to be equal to the statistical parameter *b*. b_{obsd} has been evaluated by the experimental pentad distribution in the frame of enantiomorphic site control.[37]

The Arrhenius plot of ln[$b/(1-b)$] versus $1/T_p$ yields straight lines of slope $\Delta\Delta E^{\ddagger}/R$, from which the values of enantioface selectivity $\Delta\Delta E^{\ddagger} = |\Delta E^{\ddagger}_{si} - \Delta E^{\ddagger}_{re}|$ are estimated (Scheme 4).

The ln[$b/(1-b)$] versus $1/T_p$ plots give the values of enantioface selectivity for **1**/MAO ($\Delta\Delta E^{\ddagger}_{enant}$ = 3.3 kcal/mol), **2**/MAO ($\Delta\Delta E^{\ddagger}_{enant}$ = 2.8 kcal/mol), **3**/MAO ($\Delta\Delta E^{\ddagger}_{enant}$ = 1.9 kcal/mol), **4**/MAO ($\Delta\Delta E^{\ddagger}_{enant}$ = 4.6 kcal/mol), and **5**/MAO ($\Delta\Delta E^{\ddagger}_{enant}$ = 2.6 kcal/mol). The ln[$b/(1-b)$] versus $1/T_p$ plots for **2**, **4**, and **5** are shown in Figure 5.

The $\Delta\Delta E^{\ddagger}$ values for **1** and **2** are intermediate between that of enantiomorphic site control of highly isospecific Ti catalysts (4.8 kcal/mol) and that of chain end control (ca. 2 kcal/mol).[43,44]

The lower isospecificity of **3** compared to **1** and **2** is easily accounted for by the lesser steric difference between the facing methyl and benzene rings in the former, compared to hydrogen

(41) Kissin, Y. V. *Isospecific Polymerization of Olefins*; Springer-Verlag: New York, 1985, Chapter I, p 71.

(42) Drögemüller, H.; Niedoba, S.; Kaminsky, W. *Polym. React. Eng.* **1986**, 299.

(43) Zambelli, A.; Locatelli, P.; Zannoni, G.; Bovey, F. A. *Macromolecules* **1978**, *11*, 923.

(44) Resconi, L.; Abis, L.; Franciscono, G. *Macromolecules* **1992**, *25*, 6814. Erker, G.; Fritze, C. *Angew. Chem., Int. Ed. Engl.* **1992**, *31*, 199.

Scheme 4. Schematic Representation of the Origin of $\Delta\Delta E^{\ddagger}$ in (*R*,*R*)**1**

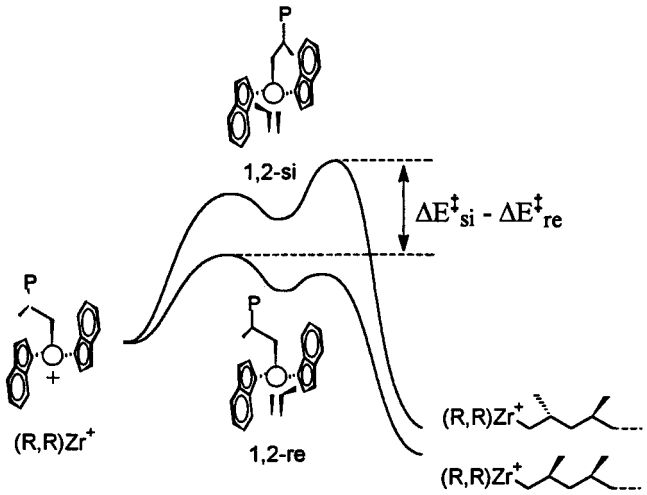

and benzene in the latter. Assuming the 3-R group to prevail over the benzene ring, Guerra's model predicts opposite enantioface selectivities for catalysts **3**−**5** with respect to the other *C*$_2$-*symmetric* systems with 3-R = H.[24]

The higher isospecificity of **4** compared to **1**−**3** is remarkable. We ascribe the lower isospecificity of **5**, compared to that of **4**, to subtle differences in their molecular structures: in fact (see X-ray section) the ^{t}Bu group is closer to the Zr center than is the Me_3Si group, due to the longer C(3)−Si bond versus the C(3)−C_{tBu} bond.

Conclusions

We have described novel, readily available, highly regiospecific zirconocenes that produce iPP with variable isotacticity, from low to medium-high, correspondingly variable melting points and very low xylene-soluble fractions. These zirconocenes are characterized by having a bisindenyl ansa ligand with bulky substituents in the 3 position and a single carbon bridge.

The influence of polymerization temperature, investigated by polymerizing propene in *liquid propene* in the temperature range of 20−70 °C, on catalyst performances is reported. *rac*-$Me_2C(3\text{-}^tBu\text{-}1\text{-}Ind)_2ZrCl_2$ (**4**) produces iPP with $\Delta\Delta E^{\ddagger}_{enant}$ = 4.6 kcal/mol (*mmmm* ca. 95%, T_m = 152 °C at T_p = 50 °C) and no detectable 2,1 units, versus $\Delta\Delta E^{\ddagger}_{enant}$ = 2.8 kcal/mol (*mmmm* ca. 81%, T_m = 127 °C) and $2,1_{tot}$ = 0.4% for *rac*-$Me_2C(1\text{-}Ind)_2ZrCl_2$/MAO and $\Delta\Delta E^{\ddagger}_{enant}$ = 3.3 kcal/mol (*mmmm* ca. 87%, T_m = 134 °C) and $2,1_{tot}$ = 0.6% for *rac*-$C_2H_4(1\text{-}Ind)_2$-$ZrCl_2$/MAO.

The salient features of catalysts **4** and **5** are the following:

(a) The zirconocenes can be prepared in acceptable yields with a simple protocol. Their ligands can be prepared with a very simple and inexpensive one-pot reaction, and a large variety of substituents can be used. From this standpoint, zirconocenes of this class are far simpler and more versatile than most other zirconocene types.

(b) Polymerization activities (MAO as cocatalyst) are good.

(c) Although the meso isomer is obtained along with, and very difficult to separate from, the racemic one in the zirconocene synthesis, the meso isomer is *inactive* (also in the case of ethylene polymerization, its activity is negligible). This is an added advantage compared to other zirconocene types.

(d) Both molecular weights and melting points are quite high compared to class I systems: intrinsic viscosities > 1 dL/g and T_m > 150 °C can be achieved at $T_p \leq$ 40 °C. iPP melting points reflect the microstructure of the samples and are in line with values previously reported for other catalyst systems.[6]

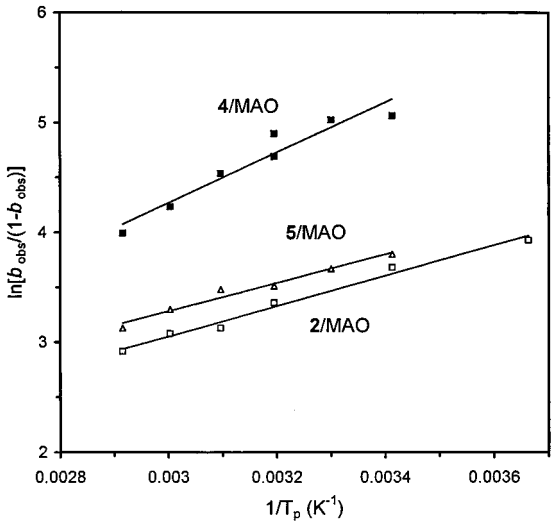

Figure 5. Arrhenius plot of $\ln[b_{obsd}/(1 - b_{obsd})]$ versus $1/T_p$ for **2**, **4**, and **5**: (□) **2**/MAO, $\Delta\Delta E^{\ddagger}$ = 2.8 ± 0.2 kcal/mol, R = 0.993; (■) **4**/MAO, $\Delta\Delta E^{\ddagger}$ = 4.6 ± 0.6 kcal/mol, R = 0.96; (△) **5**/MAO, $\Delta\Delta E^{\ddagger}$ = 2.6 ± 0.2 kcal/mol, R = 0.99. The $\Delta\Delta E^{\ddagger}$ values are obtained with the assumption that $b_{obsd} = b$, that is, with negligible epimerization (see text).

(e) Compounds **4** and **5** are much more regiospecific than **1** and **2**.

Although we are still unable to produce all industrial iPP grades at conventional (60−80 °C) polymerization temperatures, this new class of zirconocene catalysts once more demonstrates the enormous variability of metallocene catalysts and the importance of ligand design in optimizing catalyst performance. The increase in isospecificity and the decrease of chain transfer rates observed with **4** in comparison to its Si-bridged analogue[8] are noteworthy.

Experimental Section

General Procedures. Zirconocenes **1**,[3] **2**,[14] and **3**[26] were prepared according to published procedures.

Synthesis of Isopropylidenebis(3-tert-butylindenyl)zirconium Dichloride (4). Dilithium isopropylidenebis(3-*tert*-butylindenyl) (7.92 mg, (20 mmol) was suspended in 40 mL of ether and, cooled to −40 °C, and 5.0 g (42 mmol) of trimethyltin chloride was then added. The resulting mixture was allowed to warm to room temperature; the organic layer was then separated off and evaporated to give yellow oil that crystallizes under standing. It represents the mixture of *rac*-/*meso*-bis-trimethylstannylated isopropylidenebis(3-*tert*-butylindene) (*meso*-**6**/*rac*-**6**) with small contamination of Me_3SnCl. The rac/meso ratio depends heavily on the method of the initial dilithium salt crystallization and usually averages 1.5−2.0:1.

^{1}H NMR (C_6D_6, 30 °C, δ, ppm). *rac*-**6**: 7.8−7.1(some groups of multiplets, 8H), 6.82 (s, 2H), 1.92 (s, 6H), 1.26 (s, 18H), 0.03 (s, 18H). *meso*-**6**: 7.8−7.1 (some groups of multiplets, 8H), 6.70 (s, 2H), 2.06 (s, 3H), 1.92 (s, 3H), 1.20 (s, 18H), 0.00 (s, 18H). Anal. Calcd for $C_{35}H_{52}Sn_2$: C, 59.19; H, 7.38. Found: C, 58.78; H, 7.12.

The distannylated derivative thus obtained was diluted in 50 mL of toluene. Subsequently, 4.66 g (20 mmol) of $ZrCl_4$ was added, and the mixture thus obtained was taken to 80 °C and stirred for an additional 6 h. The red solution was then separated off and the toluene and Me_3-SnCl were removed under reduced pressure (10^{-2} Torr) to give 9.8 g (90%) of red crystalline solid representing *rac*-**4**/*meso*-**4** (by NMR). The product was then recrystallized from DME. Pure *rac*-isopropylidenebis(3-*tert*-butylindenyl)zirconium dichloride (4.13 g, 38%) was thus obtained. The mother liquor was collected and evaporated. The

Table 11. Crystal Data, Data Collection, Structure Solution, and Refinement Parameters

compd	**4**	**5**
emp form	$C_{29}H_{34}Cl_2Zr\cdot(C_2H_5)_2O$	$C_{27}H_{34}Cl_2Si_2Zr$
form wt	590.75	576.84
color, habit	red, plate	orange, block
cryst size, mm	0.27 × 0.36 × 0.09	0.40 × 0.40 × 0.25
cryst syst	monoclinic	orthorhombic
space group	$P2_1/c$	Pcan
unit cell dimens		
a, Å	12.458(4)	9.2356(2)
b, Å	9.514(4)	15.4522(3)
c, Å	24.584(8)	19.7476
a, deg	90	90
b, deg	100.20(3)	90
γ, deg	90	90
vol, Å^3	2868(2)	2818.19(8)
Z	4	4
density (calcd), g/cm^3	1.368	1.360
abs coeff, mm^{-1}	0.591	0.678
F(000)	1232	1192
diffractometer	Enraf-Nonius CAD-4	Siemens SMART
temp, K	293	150.0(2)
radiation, (λ, Å)	graphite monochromatized Mo Kα (0.710 73)	graphite monochromatized Mo Kα (0.710 73)
scan mode	ω	ω
scan width/scan step, deg	1.2 + 0.35 tan θ	0.3
scan rate, deg/min or time per step (min)	2/8	15
θ range, deg	4.97 to 26.96	2.06 to 27.50
index ranges	$-15 \le h \le 2$ $0 \le k \le 12$ $-29 \le l \le 31$	$-10 \le h \le 11$ $-20 \le k \le 14$ $-24 \le l \le 25$
reflns coll	3792	19209
indep reflns	3792 [R(int) = 0.0000]	3233 [R(int) = 0.0339]
absn corrn	empirical (ψ scan)	empirical (SHELXTL-Plus)
min/max transm.	0.8216/0.8736	0.61366/0.67699
decay corrn	none	none
solution method	direct methods(SHELX-86)	direct methods(SHELX-86)
refinement method	full-matrix least-squares on F^2 (SHELXL-93)	
hydrogen treatment	all H atoms were placed in calculated positions and refined using riding model	all H atoms were found objectively and refined isotropically
data/restraints/params	3792/0/310	3223/0/215
goodness-of-fit on F^2	0.969	1.113
final R indices [$I > 2\sigma(I)$]	R_1 = 0.0533, wR_2 = 0.1230	R_1 = 0.0236, wR_2 = 0.0537
R indices (all data)	R_1 = 0.1087, wR_2 = 0.1415	R_1 = 0.0298, wR_2 = 0.0599
extinct coeff	0.0000(8)	0.0008(2)
largest diff. peak and hole, e A^{-3}	0.507 and −0.468	0.356 and −0.425

residual solid was recrystallized from ether, and 2.72 g (25%) of pure *meso*-isopropylidenebis(3-*tert*-butylindenyl)zirconium dichloride was isolated.

^{1}H NMR (CD_2Cl_2, 30 °C, δ, ppm). *rac*-**4**: 7.74 ("t", 4H), 7.25 (dd, 2H), 6.97 (dd, 2H, C_6 ring), 5.97 (s, 2H, C_5 ring), 2.33 (s, 6H, >CMe_2), 1.37 (s, 18H, −CMe_3). *meso*-**4**: 7.95 ("d", 2H), 7.70 ("d", 2H), 7.04 (dd, 2H), 6.80 (dd, 2H, C_6 ring), 5.81 (s, 2H, C_5 ring), 2.67 (s, 3H, >CMe_2), 2.09 (s, 3H, >CMe_2), 1.47 (s, 18H, −CMe_3). Anal. Calcd for $C_{29}H_{34}ZrCl_2$: C, 63.94; H, 6.29. Found: C, 63.70; H, 6.21.

Synthesis of Isopropylidenebis(3-(trimethylsilyl)indenyl)zirconium Dichloride (5). 2,2-bis(1-(trimethylsilyl)inden-3-yl)propane (8.34 g, 20 mmol) was dissolved in 100 mL of ether. The solution thus obtained was cooled to −20 °C, and 22 mL of a 2.0 M solution of *n*-BuLi in pentane was added to give a suspension of dilithium 2,2-bis(3-(trimethylsilyl)inden-1-yl)propane. To this suspension, which was first allowed to rise to room temperature and was then cooled to −40 °C, 5.0 g (42 mmol) of trimethyltin chloride was added. The organic layer was separated off, and evaporated to give a mixture of *rac*-/*meso*-isopropylidenebis(1-(trimethylsilyl)-1-(trimethylstannyl)-3-indene) as yellow oil that crystallizes upon standing. The product is contaminated with a small amount of Me_3SnCl. The rac/meso ratio usually averages 1.0−1.2:1.

^{1}H NMR (C_6D_6, 30 °C, δ, ppm). *rac*-**7**: 7.71−6.98 (some groups of multiplets, 8H), 6.65 (s, 2H), 1.96 (3, 6H), 0.07 (s, 18H), −0.07 (s, 18H). *meso*-**7**: 7.71−6.98 (some groups of multiplets, 8H), 6.62 (s, 2H), 2.01(s, 3H), 1.95(s, 3H), 0.04(s, 18H), −0.03 (s, 18H). Anal. Calcd for $C_{33}H_{52}Si_2Sn_2$: C, 53.39; H, 7.06. Found: C, 52.96; H, 6.81.

The distannylated derivative thus obtained was dissolved in 50 mL of toluene, 4.66 g (20 mmol) of $ZrCl_4$ was added, and the resulting mixture was heated to 80 °C and stirred for an additional 6 h. The red solution was then separated off and the toluene and Me_3SnCl were removed under reduced pressure (10^{-2} Torr) to give 10.0 g (87%) of red crystalline solid representing *rac*-**5**/*meso*-**5** (by NMR). The product was then recrystallized from DME. Pure *rac*-isopropylidenebis(3-(trimethylsilyl)-1-indenyl)zirconium dichloride (3.69 g, 36%) was thus obtained. The mother liquor was collected and evaporated. The residual solid was recrystallized from ether, and 2.17 g (21%) of pure *meso*-isopropylidenebis(3-(trimethylsilyl)indenyl)zirconium dichloride was isolated.

^{1}H NMR (CD_2Cl_2, 30 °C, δ, ppm). *rac*-**5**: 7.80 ("d", 2H), 7.55 ("d", 2H), 7.30 (t, 2H), 7.06 (t, 2H, C_6 ring), 6.08 (s, 2H, C_5 ring), 2.37 (s, 6H, >CMe_2), 0.26 (s, 18H, −$SiMe_3$). *meso*-**5**: 7.92 ("d", 2H), 7.49 ("d", 2H), 7.10 (t, 2H), 6.88 (t, 2H, C_6 ring), 6.00 (s, 2H, C_5 ring), 2.68 (s, 3H, >CMe_2), 2.19 (s, 3H, >CMe_2), 0.35 (s, 18H, −$SiMe_3$).

Anal. Calcd for $C_{27}H_{34}Si_2ZrCl_2$: C, 56.21; H, 5.94. Found: C, 56.04; H, 5.88.

Synthesis of Isopropylidenebis(4,5,6,7-tetrahydro-3-*tert*-butylindenyl)zirconium Dichloride (4-H$_4$). *rac*-$Me_2C(3\text{-}^t\text{Bu-Ind})_2ZrCl_2$ (0.66 g) was dissolved in 50 mL of CH_2Cl_2 (red solution) and hydrogenated with H_2 (5 atm)/PtO_2 (40 mg) for 4 h. The mixture turned yellow

Table 12. Selected Bond Lengths (Å) and Angles (deg) for **4**

Bonds			
Zr(1)−Cl(1)	2.405(2)	Zr(1)−Cl(2)	2.416(2)
Zr(1)−C(1)	2.439(6)	Zr(1)−C(1′)	2.425(6)
Zr(1)−C(2)	2.446(6)	Zr(1)−C(2′)	2.462(5)
Zr(1)−C(3)	2.615(5)	Zr(1)−C(3′)	2.634(5)
Zr(1)−C(4)	2.660(6)	Zr(1)−C(4′)	2.675(6)
Zr(1)−C(9)	2.539(7)	Zr(1)−C(9′)	2.510(7)
C(1)−C(14)	1.560(8)	C(1′)-C(14)	1.519(9)
C(1)−C(2)	1.431(9)	C(1′)-C(2′)	1.435(8)
C(1)−C(9)	1.408(9)	C(1′)-C(9′)	1.426(9)
C(2)−C(3)	1.411(9)	C(2′)-C(3′)	1.416(10)
C(3)−C(4)	1.424(8)	C(3′)-C(4′)	1.418(9)
C(4)−C(9)	1.446(8)	C(4′)-C(9′)	1.441(10)
C(3)−C(10)	1.552(8)	C(3′)-C(10′)	1.541(9)
C(14)−C(15)	1.51(1)	C(14)−C(15′)	1.53(1)
Angles			
C(1)−C(2)-C(3)	109.6(6)	C(1′)-C(2′)-C(3′)	111.1(6)
C(2)−C(3)-C(4)	107.5(5)	C(2′)-C(3′)-C(4′)	106.2(6)
C(2)−C(3)-C(10)	124.6(5)	C(2′)-C(3′)-C(10′)	125.4(6)
C(4)−C(3)-C(10)	126.9(5)	C(4′)-C(3′)-C(10′)	127.3(7)
C(3)−C(4)-C(9)	107.4(6)	C(3′)-C(4′)-C(9′)	108.6(6)
C(1)−C(9)-C(4)	108.6(5)	C(1′)-C(9′)-C(4′)	108.7(6)
C(9)−C(1)-C(2)	106.9(5)	C(9′)-C(1′)-C(2′)	105.3(5)
C(2′)-C(1′)-C(14)	123.3(6)	C(2′)-C(1′)-C(14)	123.3(6)
C(9′)-C(1′)-C(14)	129.2(5)	C(9′)-C(1′)-C(14)	129.2(5)
C(1′)-C(14)−C(1)	100.1(5)	C(15)−C(14)-C(15′)	107.2(6)
C(1)−C(14)-C(15)	111.0(5)	C(1′)-C(14)−C(15′)	111.1(5)
C(1)−C(14)-C(15′)	113.5(6)	C(1′)-C(14)−C(15)	114.0(6)
Cl(1)−Zr(1)-Cl(2)	98.69(9)		

after 3 h. After filtration, the solution was brought to dryness under reduced pressure, and the solid was washed with Et_2O (2 × 5 mL) and hexane (5 mL) to yield, after drying in vacuo, 0.22 g of pure (by ^{1}H NMR) *rac*-Me_2C(4,5,6,7-tetrahydro-3-^{t}Bu-Ind)$_2ZrCl_2$.

X-ray Structure Determination and Refinements. Crystals suitable for X-ray diffraction of both compounds were grown from Et_2O.

The details of the X-ray experiment and crystallographic parameters are given in Table 11.

Both structures were solved by direct methods and refined by full-matrix least-squares on F^2. For **4**, difference Fourier synthesis shows several electron density peaks in the vicinity of the symmetry center. These peaks corresponds to disordered (C_2H_5)O solvate molecule. A pattern of disordering is rather complicated. For this reason, we considered as carbon atoms only three highest peaks that were well refined and gave relatively low isotropic thermal parameters. The final least-squares refinement was performed in the anisotropic approximation for the non-hydrogen atom of the complex molecule and in the isotropic approximation for three atoms of the solvate molecule. The hydrogen atoms were refined using the ridding model with U_{iso} equal to 1.5 of the parent carbon atom.

In crystals of **5**, the molecule occupies a special position at a 2-fold axis, which passes through the Zr and C_{br} atoms. In this structure, all of the hydrogen atoms were found from the difference Fourier synthesis. They were included in the final structure refinement in the isotropic approximation. For both structures, the highest electron density residual peaks are located in the vicinity of Zr; for **4**, they are also located in the area of the solvate molecule.

All of the calculations were performed using SHELXS86[45] and SHELX93[46] software. The ORTEP program[47] (probability 0.5) was used for drawing the molecule. Non-hydrogen atom atomic coordinates and equivalent isotropic displacements are given in the Supporting Information; Tables 12 and 13 give selected bond lengths and bond angles.

Polymerizations. Polymerization grade propene and hexane were received directly from the Montell Ferrara plant. MAO was a commercial product (Witco, 30% w/w in toluene) treated in vacuo to remove most of the unreacted TMA, or modified MAO (Albemarle) was used as received.

Table 13. Selected Bond Lengths (Å) and Angles (deg) for **5**

Bonds			
Zr(1)−Cl(1)	2.4205(4)	C(2)−C(3)	1.422(2)
Zr(1)−C(1)	2.452(2)	C(3)−C(4)	1.432(2)
Zr(1)−C(2)	2.451(2)	C(4)−C(9)	1.443(2)
Zr(1)−C(3)	2.582(2)	C(10)−C(11)	1.537(3)
Zr(1)−C(4)	2.646(1)	C(3)−Si(1)	1.874(2)
Zr(1)−C(9)	2.556(1)	Si(1)−C(12)	1.872(2)
C(1)−C(10)	1.537(2)	Si(1)−C(13)	1.863(2)
C(1)−C(2)	1.423(2)	Si(1)−C(14)	1.865(2)
C(1)−C(9)	1.441(2)		
Angles			
C(1)−C(2)−C(3)	111.8(1)	C(2)−C(1)−C(10)	123.3(1)
C(2)−C(3)−C(4)	105.1(1)	C(9)−C(1)−C(10)	128.4(1)
C(2)−C(3)−Si(1)	127.4(1)	C(1)−C(10)−C(1A)	99.4(2)
C(4)−C(3)−Si(1)	126.2(1)	C(1)−C(10)−C(11)	114.2(1)
C(3)−C(4)−C(9)	109.5(1)	C(1)−C(10)−C(11A)	110.8(1)
C(1)−C(9)−C(4)	107.5(1)	Cl(1)−Zr−Cl(2)	100.69(2)
C(9)−C(1)−C(2)	106.0(1)		

The polymerization experiments were carried out in a 1 or 2 L stainless steel autoclave with 0.4 or 1 L liquid propene for 1 h. Stirring was kept at 800 rpm by means of a three-blade propeller. Metallocene and MAO were precontacted for 10 min in toluene solution (10 mL) and then added to the monomer at 2−5 °C below the polymerization temperature, which was reached in 1−5 min. The polymerizations were quenched with CO; the polymers were isolated by venting unreacted monomer and drying in an oven under vacuum at 60 °C.

Polymer Analysis. The ^{1}H NMR spectra were acquired on a Bruker DPX-400 spectrometer operating in the Fourier transform mode at 120 °C at 400.13 MHz, with a 45° pulse and 5 s of delay between pulses; 256 or 512 transients were stored for each spectrum. The ^{13}C NMR spectra were acquired on a Bruker DPX-400 (100.61 MHz, 90° pulse, 12 s delay between pulses) or DRX-500 (125.76 MHz, 90° pulse, 16 s delay between pulses) spectrometers; about 3000 transients were stored for each spectrum. The samples were prepared by dissolving 50−100 mg of the polymer under nitrogen in 0.5 mL of degassed $C_2D_2Cl_4$. As a reference, the residual peak of C_2DHCl_4 in the ^{1}H spectra (5.95 ppm) and the peak of the *mmmm* pentad in the ^{13}C spectra (21.8 ppm) were used. The microstructure analysis (pentad distribution, type and amount of regioirregular units, and end group analysis) was carried out as previously described.[37]

The average viscosity molecular weights were obtained from the experimental intrinsic viscosities using the correlations reported in the literature for iPP[48] and aPP.[49]

Acknowledgment. We are indebted to all of the Montell people who, over several years, provided the excellent data for this work: M. Colonnesi and S. Tartarini for the polymerization experiments, D. Balboni for the synthesis of *rac*-Me_2C(4,5,6,7-tetrahydro-3-^{t}Bu-Ind)$_2ZrCl_2$, A. Marzo and L. Rimessi for the viscosity measurements, and I. Giulianelli for the DSC analysis. We thank Dr. E. Albizzati for his continual encouragement and stimulus. I.E.N. acknowledges receipt of grant 96-15-96997 from the President of Russia and Montell for support of this work.

Supporting Information Available: A listing of bond distances and bond angles, anisotropic thermal parameters, hydrogen-atom coordinates for **4** and **5** (16 pages). See any current masthead page for ordering and Internet access instructions.

JA973160S

(45) Sheldrick, G. M. *Acta Crystallogr.* **1990**, *A46*, 467.

(46) Sheldrick, G. M. SHELXL93, Program for the Refinement of Crystal Structures; University of Göttingen, Germany.

(47) Johnson, C. K. ORTEP, Report ORNL-3794, 2nd revision; Oak Ridge National Laboratory, TN, 1970.

(48) Moraglio, G.; Gianotti, G.; Bonicelli, U. *Eur. Polym. J.* **1973**, *9*, 693.

(49) Pearson, D.; Fetters, L.; Younghouse, L.; Mays, J. *Macromolecules* **1988**, *21*, 478.